

Multiscalar Critical Models with Localised Cubic Interactions

Sabine Harribey,^a William H. Pannell,^b and Andreas Stergiou^{b,c}

^a*NORDITA, Stockholm University and KTH Royal Institute of Technology,
Hannes Alfvéns väg 12, SE-106 91 Stockholm, Sweden*

^b*Department of Mathematics, King's College London, Strand, London WC2R 2LS, United Kingdom*

^c*Theoretical Physics Department, CERN, 1211 Geneva 23, Switzerland*

Interface localised interactions are studied for multiscalar universality classes accessible with the perturbative ε expansion in $4 - \varepsilon$ dimensions. The associated beta functions at one loop and partially at two loops are derived, and a wide variety of interface conformal field theories (CFTs) is found, even in cases where the bulk universality class is free or as simple as the Wilson–Fisher description of the $O(N)$ model. For up to three scalar fields in the bulk, interface fixed points are classified for all bulk universality classes encountered in this case. Numerical results are obtained for interface CFTs that exist for larger numbers of multiscalar fields. Our analytic and numerical results indicate the existence of a vast space of interface CFTs, much larger than the space of defect CFTs found for line and surface defect deformations of multiscalar models in $4 - \varepsilon$ dimensions. In this vast space, stable interfaces found for free and $O(N)$ bulks belong to the F_4 family, with global symmetries $SO(3)$, $SU(3)$, $Sp(6)$ and F_4 , realised with $N = 5, 8, 16, 24$ scalar fields, respectively.

July 2024

sabine.harribey@su.se, william.pannell@kcl.ac.uk, andreas.stergiou@kcl.ac.uk

Contents

1. Introduction	1
2. Model and beta functions	3
3. Analytic results	7
3.1. Free bulk	7
3.2. $O(N)$ bulk	9
3.3. Stability matrix	10
4. Numerical results for low values of N	11
4.1. $N \leq 3$	11
4.2. Larger numbers of fields	23
5. Conclusion	27
Appendix A. Preliminary two-loop results	28
A.1. Computation of bulk-defect integrals	31
A.1.1. Graphs with only one interface coupling	31
A.1.2. Graphs with more than one interface coupling	32
References	33

1. Introduction

The $O(N)$ vector model constitutes one of the most thoroughly studied class of conformal field theories (CFTs). While it does not appear to be exactly solvable by analytic means, there exist numerous methods to study it, such as the ε expansion [1], the $1/N$ expansion [2, 3], and the conformal bootstrap [4–6]. The ε expansion is of particular importance, as it can also be used to study a variety of CFTs reached as endpoints of renormalisation group (RG) flows triggered by operators that break $O(N)$ symmetry. Indeed, generalising to quartic multiscalar models, it is possible to seek RG fixed points for different global symmetries, which are potentially relevant for second-order phase transitions observed in various physical systems. Extensive discussions of such fixed points can be found in [7–10]. In this work we will be interested in RG flows and CFTs that emerge when these fixed points are deformed by localised cubic interactions.

The study of systems with defects has a long history and renewed attention has been devoted to them recently. Defect deformations of CFTs give rise to new types of CFTs, called defect CFTs (dCFTs), that realise conformal symmetry in dimension given by that of the defect. This commonly includes dimension one, realised on line defects, but dimension two and the associated

surface defects have also been widely discussed. Theoretical work outlining in detail the effects of the presence of defects and the observables that they give rise to can be found in [11] for boundaries and interfaces and [12] for more general defects. Such studies are of course motivated by the fact that defects describe numerous physical situations, such as the presence of impurities and localised perturbations, that can be realised experimentally; see for example [13–19].

For the three-dimensional $O(N)$ model, numerous studies have been carried out for boundaries and defects. Such research dates back many years [20–22, 11, 23], and more recently novel universality classes were determined for surface defects with quartic interactions in the bulk in exactly three dimensions [24–27].

Looking beyond the $O(N)$ model, RG properties of multiscalar models with defects open up an array of new research directions, as various fixed points can be found breaking the bulk symmetry in different ways. Besides their theoretical interest, such studies also have experimental applications. For example, in dimension three the cubic and Heisenberg model are famously hard to distinguish as their most easily accessible critical exponents are nearly identical; see e.g. [7]. However, if the presence of a defect or interface breaks the bulk global symmetries in different ways, these two models could be distinguished without resorting to measurements of bulk critical exponents. This idea was explored in [28], where a line defect perturbing a quartic multiscalar model was studied. In the case of an $O(N)$ bulk, a line defect can only break the bulk symmetry to $O(N - 1)$. However, more complicated bulk symmetries, such as hypercubic or hypertetrahedral, allow for different patterns of symmetry breaking on a line defect. This fact, along with new observables that arise for a CFT in the presence of a defect, enable new computations and characterisations of bulk universality classes. Beyond line defects, [29–31] studied a surface defect perturbing the quartic $O(N)$ model and found that the bulk symmetry can only be broken to $O(p) \times O(N - p)$ with $p < N$ at leading order in the ε expansion.

Here we will go one step further and study a defect with interactions cubic in the scalar field ϕ . In this case we do not fix the dimension of the defect but its co-dimension. More specifically, we consider a co-dimension one defect, representing an interface. Our considerations generalise those of [32], where the bulk symmetry was fixed to $O(N)$ and the interface symmetry to $O(N - 1)$. Our deformation takes the general form

$$S_{\text{interface}} = \int d^{3-\varepsilon} \mathbf{x} \frac{1}{3!} h_{ijk} \phi_i \phi_j \phi_k, \quad i, j, k = 1, \dots, N, \quad (1.1)$$

where ϕ_i are scalar fields and h_{ijk} are defect couplings. We add this deformation to $(4 - \varepsilon)$ -dimensional bulk CFTs with various global symmetry groups. We then study fixed points both analytically and numerically for different values of N . Generically, we find numerous fixed points that break the bulk global symmetry to a subgroup. The possible symmetry breaking patterns we obtain are far richer than for line and surface defects. We focus on unitary fixed points, as defined by real critical values of the defect couplings, although our methods can be used to find and analyse non-unitary fixed points as well.

In the case of a free bulk, operators cubic in ϕ have dimension $3 - \frac{3}{2}\varepsilon + O(\varepsilon^2)$, which implies that the deformation (1.1) is relevant at the trivial ($h_{ijk} = 0$) defect. If we deform an interacting bulk by (1.1), however, then the $\phi_i\phi_j\phi_k$ operators will organise themselves into irreducible representations of the bulk symmetry at the trivial defect, whose dimensions may be below, at or above $3 - \varepsilon$ at order ε . Therefore, such deformations localised on an interface may be relevant, marginal or irrelevant at leading order. Regardless of their relevance in the RG sense, they can all be analysed perturbatively and we will indeed consider below deforming operators that include marginal and irrelevant ones. In essence, we are exploring the space of nontrivial interfaces that lie perturbatively close to the trivial one.

In that space, we typically find interacting interface fixed points with relevant operators cubic in ϕ . These fixed points are thus RG unstable. For free and $O(N)$ bulks, however, we find that the F_4 family [33] gives interacting interfaces that are RG stable, realising $SO(3)$, $SU(3)$, $Sp(6)$ and F_4 global symmetry with $N = 5, 8, 16, 24$ scalar fields, respectively. (To be precise, by RG stable we mean that the symmetry-preserving cubic in ϕ deformations localised on the interface are irrelevant. Of course ϕ^2 localised on the interface is a strongly relevant quadratic operator.) These interfaces are the only interacting RG stable ones we were able to find analytically, but others may be hiding in our numerical results.

The paper is organised as follows. In section 2, we present in more detail the model and derive the one-loop interface beta functions. In section 3, we compute fixed points analytically for specific defect and bulk symmetries. We also discuss the link between zero eigenvalues of the stability matrix and breaking of the bulk symmetry group. In section 4, we present numerical results for fixed points at low values of N and bulk symmetry $O(N)$, hypercubic, biconical and hypertetrahedral, as well as decoupled and free bulk theories. Finally, in appendix A we give (incomplete) results on the computation of the two-loop interface beta functions.

2. Model and beta functions

We will study a multiscalar model with quartic interactions in a $(d+1)$ -dimensional bulk and cubic interactions localised on a d -dimensional interface. It is a generalisation of the model studied in [32] and is defined by the action

$$S = \int d^d \mathbf{x} \int dy \left(\frac{1}{2} \partial^\mu \phi_i \partial_\mu \phi_i + \frac{1}{4!} \lambda_{ijkl} \phi_i \phi_j \phi_k \phi_l \right) + \int d^d \mathbf{x} \frac{1}{3!} h_{ijk} \phi_i \phi_j \phi_k, \quad (2.1)$$

where the indices take values from 1 to N and a summation over repeated indices is implicit. The coupling tensors λ_{ijkl} and h_{ijk} are symmetric, thus corresponding in general to $\binom{N+3}{4}$ and $\binom{N+2}{3}$ couplings, respectively. The interface interactions are marginal in dimension three, while the bulk interactions are marginal in dimension four. To allow a perturbative treatment we will thus set $d = 3 - \varepsilon$ in the following.

The propagator of the free theory is given by

$$\langle \phi_i(x_1)\phi_j(x_2) \rangle = \delta_{ij} \int \frac{d^{d+1}x}{(2\pi)^{d+1}} \frac{e^{ip \cdot x_{12}}}{p^2} = \delta_{ij} \frac{C_\phi}{|x_{12}|^{d-1}}, \quad C_\phi = \frac{\Gamma\left(\frac{d-1}{2}\right)}{4\pi^{\frac{d+1}{2}}}, \quad x_{12} = x_1 - x_2. \quad (2.2)$$

The free interface-to-bulk propagator K_{ij} and the free interface propagator G_{ij} in momentum space are obtained by Fourier-transforming the parallel but not the perpendicular coordinates to the defect. They were computed in [32] and they are given by

$$K_{ij}(\mathbf{p}, y) = \delta_{ij} \frac{e^{-|\mathbf{p}||y|}}{2|\mathbf{p}|}, \quad G_{ij}(\mathbf{p}) = \delta_{ij} \frac{1}{2|\mathbf{p}|}. \quad (2.3)$$

We will compute the beta functions in dimensional regularisation in $d = 3 - \varepsilon$ using the minimal subtraction scheme. As is standard, renormalised fields are defined by $\phi_{i,B} = (Z^{1/2})_{ij} \phi_{j,R}$, where the subscripts B and R denote bare and renormalised, respectively. (Such subscripts are omitted below, except where strictly necessary.)

The theory in the bulk will not be modified by the interface interactions. The wavefunction renormalisation factor Z_{ij} is thus the same as for the usual quartic multiscalar model, starting at two loops

$$Z_{ij} = \delta_{ij} - \frac{1}{12\varepsilon} \lambda_{iklm} \lambda_{jklm} + \mathcal{O}(\lambda^3), \quad (2.4)$$

where we have rescaled the renormalised coupling as $\lambda_{ijkl} \rightarrow 16\pi^2 \lambda_{ijkl}$. Furthermore, the beta functions for a quartic multiscalar model at one loop are given by the well-known expression

$$\beta_{ijkl} = -\varepsilon \lambda_{ijkl} + (\lambda_{ijmn} \lambda_{mnkl} + 2 \text{ perms}), \quad (2.5)$$

where the “2 perms” notation captures the two terms obtained by permuting the free indices in non-equivalent ways.

To compute the beta functions of the interface couplings we require finiteness of a three-point function in the presence of the interface. We find that this is much simpler than determining the beta function by requiring finiteness of the one-point function $\langle \phi_i \phi_j \phi_k(x) \rangle$ in the presence of the interface, as would be the natural extension of line and surface defect calculations found in the literature. More specifically, we write the bare defect coupling in terms of the renormalised one as

$$h_{ijk,B} = \mu^{\varepsilon/2} (h_{ijk,R} + \delta h_{ijk}), \quad (2.6)$$

where μ is an arbitrary mass scale that renders the renormalised coupling $h_{ijk,R}$ dimensionless. The counterterm δh_{ijk} has an expansion as a Laurent series in ε ,

$$\delta h_{ijk} = \sum_{n \geq 1} \frac{Z_{ijk}^{(n)}(h, \lambda)}{\varepsilon^n}. \quad (2.7)$$

The coefficients $Z_{ijk}^{(n)}(h, \lambda)$ can be obtained by requiring that the three-point function

$$\Gamma_{ijk}(\mathbf{p}_1, \mathbf{p}_2, \mathbf{p}_3, y) = \delta^{(d)}(\mathbf{p}_1 + \mathbf{p}_2 + \mathbf{p}_3) \langle \phi_i(\mathbf{p}_1, y) \phi_j(\mathbf{p}_2, y) \phi_k(\mathbf{p}_3, y) \rangle \quad (2.8)$$

in the presence of the defect is finite. To simplify calculations we take $\mathbf{p}_3 = \mathbf{0}$ and $\mathbf{p}_1 = -\mathbf{p}_2 = \mathbf{p}$. To extract divergences that can be absorbed into a redefinition of the defect coupling as in (2.7), it suffices to consider the amputated three-point function, whose expected form is

$$\hat{\Gamma}_{ijk} = h_{ijk,B} + \sum_{\ell \geq 1} \frac{1}{|\mathbf{p}|^{\ell \varepsilon}} \mathcal{A}_{ijk}^{(\ell)}, \quad (2.9)$$

where $\mathcal{A}_{ijk}^{(\ell)}$ is a sum of tensor structures in the bare couplings at loop order ℓ .

The diagrams contributing to the one-loop three-point function as well as their amplitudes were determined in [32]. Setting $|\mathbf{p}| = \mu$, the three-point function at one loop is given by

$$\mu^{-\varepsilon} \mathcal{A}_{ijk}^{(1)} = B(\lambda_{ijlm} h_{klm} + 2 \text{ perms}) + T h_{ilm} h_{jln} h_{kmn}, \quad (2.10)$$

where

$$B = \text{---} \text{---} \text{---} \text{---} \text{---} \text{---} = -\frac{\mu^{-\varepsilon}}{16\pi^2 \varepsilon} + \mathcal{O}(\varepsilon^0), \quad (2.11)$$

and

$$T = \text{---} \text{---} \text{---} \text{---} \text{---} \text{---} = \frac{\mu^{-\varepsilon}}{16\pi^2 \varepsilon} + \mathcal{O}(\varepsilon^0). \quad (2.12)$$

In our graphical representation, thin dashed propagators are in the bulk, thick dashed propagators are from the bulk to the defect (K in (2.3)), and solid ones are purely on the defect (G in (2.3)). Additionally, square vertices are in the bulk, while circular ones are on the defect. The counterterm $Z_{ijk}^{(1)}$ is then simply given by

$$Z_{ijk}^{(1)} = \frac{1}{16\pi^2 \varepsilon} (\lambda_{ijlm} h_{klm} + 2 \text{ perms}) - \frac{1}{16\pi^2 \varepsilon} h_{ilm} h_{jln} h_{kmn}. \quad (2.13)$$

In minimal subtraction the beta function coefficients can be read off from these simple-pole residues [34]. In particular, in our case the beta functions are given by

$$\beta_{ijk} = -\frac{\varepsilon}{2} h_{ijk} + \frac{1}{2} \left(h_{lmn} \frac{\partial}{\partial h_{lmn}} + 2 \lambda_{lmnp} \frac{\partial}{\partial \lambda_{lmnp}} - 1 \right) Z_{ijk}^{(1)}. \quad (2.14)$$

With our result (2.13) we finally obtain the one-loop interface beta function

$$\beta_{ijk} = -\frac{\varepsilon}{2} h_{ijk} + (\lambda_{ijlm} h_{klm} + 2 \text{ perms}) - \frac{1}{4} h_{ilm} h_{jln} h_{kmn}, \quad (2.15)$$

where we have rescaled the interface coupling as $h_{ijk} \rightarrow 2\pi h_{ijk}$ (and the bulk coupling as $\lambda_{ijkl} \rightarrow 16\pi^2 \lambda_{ijkl}$ as above). At this order, the beta function is gradient, i.e.

$$\beta_{ijk} = \frac{\partial H}{\partial h_{ijk}}, \quad H = -\frac{1}{4} \varepsilon h_{ijk} h_{ijk} + \frac{3}{2} \lambda_{ijkl} h_{ijm} h_{klm} - \frac{1}{16} h_{ijk} h_{ilm} h_{jln} h_{kmn}. \quad (2.16)$$

At two loops there is a variety of diagrams that contribute to the beta function. Using our graphical notation from above, these are given in Figs. 1, 2 and 3. While we have not been able

to compute all of their contributions to the interface beta function, we summarise the results we have obtained in appendix A.

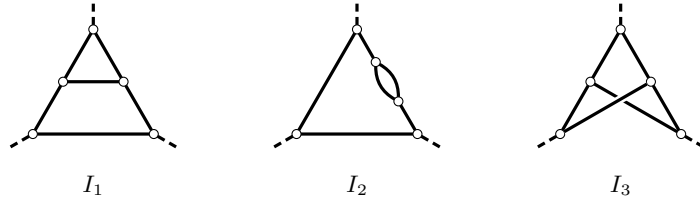


Fig. 1: Two-loop graphs with only cubic couplings

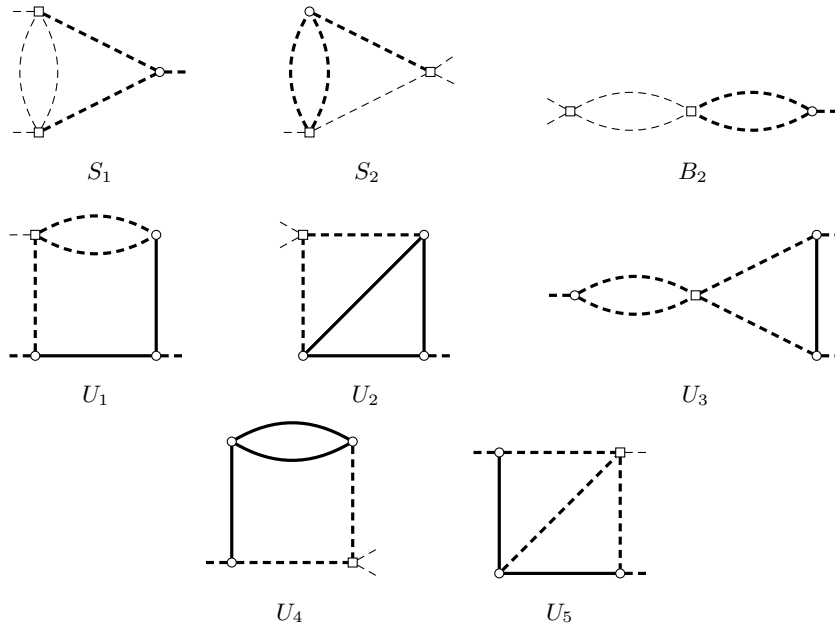


Fig. 2: Two-loop graphs with both cubic and quartic couplings.

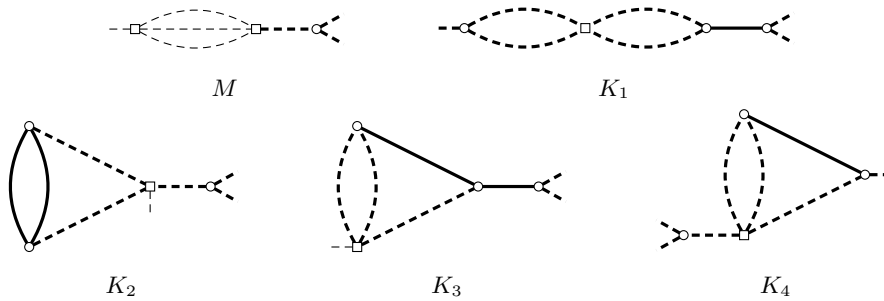


Fig. 3: One-particle reducible graphs contributing to the interface three-point function

Here we would like to mention a trick that allows the calculation of contributions to the beta function linear in the interface coupling h . At the trivial defect, $h = 0$, eigenvalues of the stability

matrix $\partial\beta/\partial h$ are directly related to the anomalous dimensions of the nearly marginal deforming operators. If the bulk theory is also free, this observation is of no use, but if it is not it sets constraints on the coefficients of the terms linear in h that appear in the defect beta function.

For example, if the bulk CFT is the $O(N)$ model and we work at one loop, then there are two linearly-independent beta functions [32] and, neglecting terms cubic in the couplings h_1, h_2 , which are irrelevant for the argument we are making here, we have

$$\beta_1 \supset \left(\frac{2\alpha - 1}{2} h_1 + \frac{\alpha}{N + 8} h_2 \right) \varepsilon, \quad \beta_2 \supset -\frac{(N + 8 - 12\alpha)}{2(N + 8)} h_2 \varepsilon, \quad (2.17)$$

where α is the beta function coefficient that follows from (2.11); $\alpha = 1$ from (2.15). The matrix $\partial\beta_a/\partial h_b$, $a, b = 1, 2$, evaluated at the trivial defect, $h_1 = h_2 = 0$, is upper-triangular and thus has the obvious eigenvalues

$$\kappa_1 = \left(\alpha - \frac{1}{2} \right) \varepsilon, \quad \kappa_2 = -\frac{N + 8 - 12\alpha}{N + 8} \varepsilon. \quad (2.18)$$

These eigenvalues then determine the scaling dimensions of bulk operators one uses to deform away from the trivial defect. In our case these are cubic operators in particular $O(N)$ irreps, namely vector and three-index traceless symmetric, and their dimensions are known from bulk computations to be¹

$$\Delta_1 = 3 - \frac{1}{2} \varepsilon + O(\varepsilon^2), \quad \Delta_2 = 3 - \frac{3}{2} \varepsilon + \frac{6}{N + 8} \varepsilon + O(\varepsilon^2), \quad (2.19)$$

respectively [35]. Neglecting terms of order ε^2 and higher, it must be that

$$\kappa_{1,2} = \Delta_{1,2} - (3 - \varepsilon), \quad (2.20)$$

which implies that $\alpha = 1$ consistently with the explicit computation of the loop diagram (2.11).

At two loops there are four contributions to the beta function linear in $h_{1,2}$. Using the order ε^2 contributions to (2.19) given in [35] allows us to determine all four corresponding coefficients. These are otherwise given by rather complicated integrals, three of which we have not been able to evaluate analytically.

3. Analytic results

3.1. Free bulk

Fixed points of (2.15) are found by first fixing λ_{ijkl} , which corresponds to a determination of the bulk universality class. As a first example, let us choose the bulk to be free. Then, interface fixed

¹ $\Delta_1 = 4 - \varepsilon - \Delta_\phi$ corresponds to the equation of motion operator and Δ_2 to the three-index traceless symmetric of the $O(N)$ model.

points correspond to solutions of

$$\beta_{ijk} = -\frac{1}{2}\varepsilon h_{ijk} - \frac{1}{4}h_{ilm}h_{jln}h_{kmn} = 0. \quad (3.1)$$

Fixed points of this equation are not easy to analyse in full generality, so we discuss here some examples that are determined by the symmetry we would like to preserve on the interface. The bulk free theory has $O(N)$ symmetry and we may choose to preserve different subgroups of that.

The case of $O(N-1)$ on the interface was extensively analysed in [32]. It was found that for $N \leq 2$ there are no unitary fixed points, while for $N > 2$ there is one pair of physically equivalent unitary fixed points for each N . These fixed points have relevant operators, so they are unstable.

An interesting class of examples with one defect coupling arises when $h_{ijk} = \hbar d_{ijk}$, with d_{ijk} a symmetric traceless tensor. If d_{ijk} is the only such tensor and there are no primitive two-index invariant tensors beyond δ_{ij} , then we may impose

$$d_{ikl}d_{jkl} = r\delta_{ij}, \quad r > 0, \quad d_{ilm}d_{jln}d_{kmn} = s d_{ijk}, \quad (3.2)$$

and (3.1) becomes

$$\beta_{\hbar} = -\frac{1}{2}\varepsilon\hbar - \frac{1}{4}s\hbar^3 = 0, \quad (3.3)$$

which is solved for $\hbar = 0$ or

$$\hbar^2 = -\frac{2}{s}\varepsilon. \quad (3.4)$$

Unitarity requires $s < 0$. The constants r, s obey the bound [8]

$$-\frac{N-2}{2(N+2)}r \leq s \leq \frac{N-2}{N-1}r. \quad (3.5)$$

At the non-trivial interface fixed point given by (3.4) the operator $d_{ijk}\phi_i\phi_j\phi_k$ has dimension $3 + O(\varepsilon^2)$ and thus gives rise to an irrelevant perturbation when localised on the interface; this fixed point is RG stable. (At the trivial interface, $d_{ijk}\phi_i\phi_j\phi_k$ has dimension $3 - \frac{3}{2}\varepsilon + O(\varepsilon^2)$ and corresponds to a relevant perturbation when localised on the interface.)

S_{N+1} symmetry is an example of this construction. To realise it, we introduce $N+1$ vectors e_i^α , $\alpha = 1, \dots, N+1$,² satisfying

$$\sum_{\alpha} e_i^\alpha = 0, \quad \sum_{\alpha} e_i^\alpha e_j^\alpha = \delta_{ij}, \quad e_i^\alpha e_i^\beta = \delta^{\alpha\beta} - \frac{1}{N+1}. \quad (3.6)$$

Then,

$$d_{ijk} = \sum_{\alpha} e_i^\alpha e_j^\alpha e_k^\alpha \quad (3.7)$$

and one may compute [8, Appendix C]

$$r = \frac{N-1}{N+1}, \quad s = \frac{N-2}{N+1}. \quad (3.8)$$

²These vectors point to the $N+1$ vertices of an N -dimensional hypertetrahedron.

The S_{N+1} theory saturates the upper bound of (3.5). Unitarity requires $N < 2$ and so unitary S_{N+1} symmetric fixed points do not exist for a free bulk.

Another example is given by $SU(n)$ symmetry, $n > 2$, $N = n^2 - 1$, for which d_{ijk} is the standard symmetric tensor and then

$$r = \frac{n^2 - 4}{n}, \quad s = \frac{n^2 - 12}{2n}. \quad (3.9)$$

Unitary fixed points can be found for $n^2 < 12$. In particular, $n = 3$, for which $N = 8$, gives an $SU(3)$ symmetric interacting interface CFT which, as discussed above, is RG stable.

Beyond the $SU(3)$ example, there are three further examples from the F_4 family considered in [33],³ for which $N = 5$, $N = 14$ and $N = 26$, with symmetry $SO(3)$, $Sp(6)$ and F_4 , respectively. All of these, like the $SU(3)$ case, saturate the lower bound of (3.5) and thus satisfy

$$s = -\frac{N - 2}{2(N + 2)}r \quad (3.10)$$

for their respective N . Since $r > 0$, they define unitary interacting CFTs that are RG stable.

We have also sought fixed points with S_N symmetry, for which there are three independent couplings. For this case we do not have a general closed-form solution for the fixed points valid for any N . However, all unitary fixed points we have found by demanding S_N symmetry have enhanced $O(N - 1)$ symmetry.

3.2. $O(N)$ bulk

When the bulk universality class is fixed to the $O(N)$ model, then again [32] found unitary interface fixed points with $O(N - 1)$ symmetry for $2 \leq N \leq 7$ which were RG unstable, while for N outside this range there were only non-unitary interface fixed points with $O(N - 1)$ symmetry.

Considering fixed points with one rank-three symmetric traceless invariant tensor as in the previous section now gives fixed points as solutions of

$$\beta_{\hbar} = -\frac{N - 4}{2(N + 8)}\varepsilon\hbar - \frac{1}{4}s\hbar^3 = 0. \quad (3.11)$$

If $\hbar \neq 0$ this is solved for

$$\hbar^2 = -\frac{2(N - 4)}{N + 8}\frac{1}{s}\varepsilon, \quad (3.12)$$

and at this fixed point the operator $d_{ijk}\phi_i\phi_j\phi_k$ has dimension $3 - \frac{12}{N+8}\varepsilon + O(\varepsilon^2)$. RG stability requires $N > 4$ and unitarity in that case imposes $s < 0$. (At the trivial interface, $d_{ijk}\phi_i\phi_j\phi_k$ has dimension $3 - \frac{3(N+4)}{2(N+8)}\varepsilon + O(\varepsilon^2)$ and corresponds to a relevant perturbation when localised on the interface if $N > 4$.)

³Discussions of this family in different settings than considered here can be found in [36–39].

Due to (3.8), S_{N+1} symmetry on the interface can be realised on a unitary fixed point only for $N = 3$ and this fixed point is RG unstable. Unitary RG stable fixed points exist for $SO(3)$, $SU(3)$, $Sp(6)$ and F_4 symmetries, with $N = 5, 8, 14, 26$, respectively.

Requiring S_N symmetry on the interface we again find a unitary fixed point only for $N = 3$. As it turns out (see Table 6 below), for $N = 3$ the fixed points we have found, namely those with symmetry $O(2)$, S_4 and S_3 , along with two fixed points with symmetry \mathbb{Z}_2^2 , constitute the full set of unitary interface fixed points that can be obtained for an $O(3)$ bulk.

Let us remark here that for $N = 4$ the three-index traceless symmetric operator localised on an interface leads to a marginal perturbation at leading order in ε , as can be seen from Δ_2 in (2.19). Therefore, one may find a manifold of fixed points at this order. Indeed, this is the case, as there exist solutions of $\beta_{ijk} = 0$ for the beta function given in (2.15) for which the first two terms cancel and the term cubic in h can be set to zero without fixing all couplings. There are then genuine ‘‘conformal manifolds’’ at leading order, but we have checked using our two-loop results that they do not survive at next-to-leading order; for this it is enough that the contribution of the I_3 diagram in Fig. 1 to the two-loop interface beta function is non-zero.

3.3. Stability matrix

The anomalous dimensions of cubic operators at a given fixed point are given by the eigenvalues, κ , of the stability matrix

$$S_{ijk,lmn} = \frac{\partial \beta_{ijk}}{\partial h_{lmn}} \quad (3.13)$$

evaluated at the fixed point. Relevant operators correspond to $\kappa < 0$ and irrelevant operators correspond to $\kappa > 0$. The breaking of a continuous bulk symmetry group G to a subgroup $H < G$ by the introduction of the defect is associated with the existence of marginal $\kappa = 0$ eigenvalues. These arise due to the eigenvector

$$v_{ijk} = \omega_{ia} h_{ajk} + \omega_{ja} h_{aik} + \omega_{ka} h_{aij} \quad (3.14)$$

of the stability matrix. Here $\omega_{ij} = -\omega_{ji}$ and

$$\omega_{ia} \lambda_{ajkl} + \omega_{ja} \lambda_{iakl} + \omega_{ka} \lambda_{ijal} + \omega_{la} \lambda_{ijka} = 0 \quad (3.15)$$

since λ_{ijkl} is invariant under the action of G .

Examining the form of v_{ijk} , one sees that if ω_{ij} arises due to the remaining symmetry group H then $v_{ijk} = 0$, so that the statement $S_{ijk,lmn} v_{lmn} = 0$ is only non-trivial when the ω_{ij} are chosen to correspond to the generators of G broken by the defect. The number of $\kappa = 0$ eigenvalues will then equal the number of generators of the bulk symmetry group broken at the defect fixed point, allowing one to easily determine the dimension of the remaining symmetry group H .

4. Numerical results for low values of N

For N bulk scalar fields there will be a total of $N(N+1)(N+2)/3!$ independent defect beta functions one must solve in order to find fixed points. As N increases, the analytic problem becomes intractable unless we assume that the defect perturbation takes a specific form to reduce the number of independent equations. When concerned with general questions about the symmetry breaking patterns which may arise at values of N above two we must turn to numerical methods for answers. First, let us note that in extensive searches of coupling space it is essential to determine whether or not two fixed points are really distinct. The bulk tensor λ_{ijkl} will be invariant under some bulk symmetry group $G \leq O(N)$, acting via rotation on the vector indices

$$R_{ia}R_{jb}R_{kc}R_{ld}\lambda_{abcd} = \lambda_{ijkl}, \quad R \in G. \quad (4.1)$$

The introduction of a non-zero defect coupling h_{ijk} will break G to some defect symmetry group $H \leq G$. If we consider a rotation R which is in G but not in H , one can see that if $h_{1,ijk}$ is a fixed point, then so too will be

$$h_{2,ijk} = R_{ia}R_{jb}R_{kc}h_{1,abc}. \quad (4.2)$$

As the action of G on the scalar fields ϕ_i is a field redefinition $\phi_i \rightarrow \phi'_i = R_{ij}\phi_j$, the fixed points $h_{1,ijk}$ and $h_{2,ijk}$ must be physically equivalent, so that the coupling space is properly defined modulo the action of G . It is thus more useful to work not directly with the fixed points h_{ijk} one finds, but instead with the two $O(N)$ invariants

$$h^2 = h_{ijk}h_{ijk}, \quad h_i^2 = h_{ijj}h_{ikk}, \quad (4.3)$$

which are the same for each member of the orbit of h_{ijk} under G . It is with these invariants that we will characterise the fixed points we find.

To perform the numerical search itself we rely upon *Mathematica*'s `FindRoot` function. As our initial input we take random sampling of points, with $0 \leq h_{ijk} \leq 1$ for all i, j, k . To verify the convergence, we take only those solutions with error less than 10^{-10} and then demand that at higher precision an improved solution can be found with error less than 10^{-100} .

4.1. $N \leq 3$

Before considering the case of interacting bulk models, let us consider an interface placed inside of a bulk containing N free scalars. Unlike in the case of line defects, the existence of the purely defect term T in the beta function permits the existence of non-trivial solutions to $\beta_{ijk} = 0$ whilst setting $\lambda_{ijkl} = 0$. We find no solutions for a free bulk with $N \leq 2$, while we find one non-trivial fixed point arising at $N = 3$ given in Table 1.

Table 1: Fixed points found for an $N = 3$ free bulk.

Symmetry	h^2	h_i^2	$\# \kappa < 0, =0$
$O(2)$	72.5147	6.1402	7, 2

As indicated by the two $\kappa = 0$ eigenvalues, the $O(3)$ bulk symmetry is broken to an $O(2)$ symmetry on the interface, so that the fixed point lies within the $O(N-1)$ symmetry breaking family studied previously for a free bulk in [32].

Let us now take $\lambda_{ijkl} \neq 0$. For low values of N there are few fully interacting bulk critical models from which we can choose [10], and it is thus possible to engage in a complete classification of critical interface models with only a few scalar fields. For $N = 1$, the only interacting bulk point is the \mathbb{Z}_2 Wilson–Fisher fixed point, with

$$\lambda_{1111} = \frac{\varepsilon}{3}. \quad (4.4)$$

The beta function for the sole defect coupling is then given by

$$\beta_{111} = \frac{\varepsilon}{2}h_{111} - \frac{1}{4}h_{111}^3, \quad (4.5)$$

which has the unique non-trivial solution $h_{111} = \pm\sqrt{2\varepsilon}$ listed in Table 2. The introduction of the defect will completely break the \mathbb{Z}_2 symmetry in this system, reflected by the ambiguity in the choice of sign. Here, the stability matrix is simply given by the real number

$$S = \frac{\varepsilon}{2} - \frac{3}{4}h_{111}^2 = -\varepsilon. \quad (4.6)$$

As this number is negative, the corresponding cubic operator will be relevant, and the fixed point will thus be unstable.

Table 2: Fixed points found for a \mathbb{Z}_2 bulk.

Symmetry	h^2	h_i^2	$\# \kappa < 0, =0$
None	2	2	1, 0

For $N = 2$, there are now three choices of bulk critical models: a decoupled pair of Ising theories $I \times I$, a decoupled $I \times$ Free theory, and the $O(2)$ critical model. Let us first consider the former of these, where the interaction tensor can be expressed by

$$\lambda_{ijkl}\phi_i\phi_j\phi_k\phi_l = \frac{\varepsilon}{3}(\phi_1^4 + \phi_2^4), \quad (4.7)$$

which is invariant under a symmetry group $\mathbb{Z}_2^2 \times \mathbb{Z}_2$. We now have four independent defect couplings,

$$k_1 = h_{111}, \quad k_2 = h_{222}, \quad g_1 = h_{122}, \quad g_2 = h_{112}, \quad (4.8)$$

the beta functions for which are

$$\begin{aligned} \beta_{k_1} &= \frac{\varepsilon}{2}k_1 - \frac{k_1^3}{4} - \frac{g_1^3}{4} - \frac{3}{4}g_2^2(k_1 + g_1), \\ \beta_{k_2} &= \frac{\varepsilon}{2}k_2 - \frac{k_2^3}{4} - \frac{g_2^3}{4} - \frac{3}{4}g_1^2(k_2 + g_2), \\ \beta_{g_1} &= -\frac{\varepsilon}{6}g_1 - \frac{1}{4}(k_1 + g_1)(g_1^2 + g_2^2) - \frac{g_1}{4}(k_2 + g_2)^2, \\ \beta_{g_2} &= -\frac{\varepsilon}{6}g_2 - \frac{1}{4}(k_2 + g_2)(g_1^2 + g_2^2) - \frac{g_2}{4}(k_1 + g_1)^2. \end{aligned} \quad (4.9)$$

One can explicitly solve these equations to find that the only solutions are decoupled theories obtained via direct sums of the solution in Table 2, as shown in Table 3.

Table 3: Fixed points found for a decoupled $I \times I$ bulk.

Symmetry	h^2	h_i^2	$\# \kappa < 0, =0$
\mathbb{Z}_2	2	2	3, 0
\mathbb{Z}_2	4	4	4, 0

Taking the bulk to lie at the decoupled $I \times \text{Free}$ fixed point with symmetry \mathbb{Z}_2^2 , where the interaction tensor is

$$\lambda_{ijkl}\phi_i\phi_j\phi_k\phi_l = \frac{\varepsilon}{3}\phi_1^4, \quad (4.10)$$

we find the four beta functions

$$\begin{aligned} \beta_{k_1} &= \frac{\varepsilon}{2}k_1 - \frac{k_1^3}{4} - \frac{g_1^3}{4} - \frac{3}{4}g_2^2(k_1 + g_1), \\ \beta_{k_2} &= -\frac{\varepsilon}{2}k_2 - \frac{k_2^3}{4} - \frac{g_2^3}{4} - \frac{3}{4}g_1^2(k_2 + g_2), \\ \beta_{g_1} &= -\frac{\varepsilon}{2}g_1 - \frac{1}{4}(k_1 + g_1)(g_1^2 + g_2^2) - \frac{g_1}{4}(k_2 + g_2)^2, \\ \beta_{g_2} &= -\frac{\varepsilon}{6}g_2 - \frac{1}{4}(k_2 + g_2)(g_1^2 + g_2^2) - \frac{g_2}{4}(k_1 + g_1)^2. \end{aligned} \quad (4.11)$$

These may be explicitly solved, and as for the $I \times I$ theory the only resulting fixed points are obtained by direct sums of solutions for the Ising model and the $N = 1$ free theory. As the $N = 1$ free theory has no non-trivial defects, we are left with a single fixed point as shown in Table 4.

Table 4: Fixed points found for an $I \times$ Free bulk.

Symmetry	h^2	h_i^2	$\# \kappa < 0, =0$
\mathbb{Z}_2	2	2	4, 0

Considering now the $O(2)$ model, the bulk interaction tensor takes the form

$$\lambda_{ijkl} = \frac{\varepsilon}{10} (\delta_{ij}\delta_{kl} + \delta_{ik}\delta_{jl} + \delta_{il}\delta_{jk}). \quad (4.12)$$

The beta functions for the four independent couplings k_1 , k_2 , g_1 and g_2 are given by

$$\begin{aligned} \beta_{k_1} &= \frac{3\varepsilon}{10}k_1 - \frac{k_1^3}{4} - \frac{g_1^3}{4} - \frac{3}{4}g_2^2(k_1 + g_1), \\ \beta_{k_2} &= \frac{3\varepsilon}{10}k_2 - \frac{k_2^3}{4} - \frac{g_2^3}{4} - \frac{3}{4}g_1^2(k_2 + g_2), \\ \beta_{g_1} &= \frac{3\varepsilon}{10}g_1 - \frac{1}{4}(k_1 + g_1)(g_1^2 + g_2^2) - \frac{g_1}{4}(k_2 + g_2)^2, \\ \beta_{g_2} &= \frac{3\varepsilon}{10}g_2 - \frac{1}{4}(k_2 + g_2)(g_1^2 + g_2^2) - \frac{g_2}{4}(k_1 + g_1)^2. \end{aligned} \quad (4.13)$$

These expressions may be solved numerically to yield the three non-trivial fixed points listed in Table 5. Importantly, it is possible to use the bulk $O(2)$ symmetry to rewrite the deformation h_{ijk} at these fixed points in the simple form

$$h_{ijk}\phi_i\phi_j\phi_k = 3\lambda_1\phi_2\phi_1^2 + \lambda_2\phi_2^3, \quad (4.14)$$

so that these fixed points fall into the family of fixed points classified previously in [32]. As one can see from the form of the potential and the number of $\kappa = 0$ eigenvalues, these fixed points break the bulk $O(2)$ symmetry to a \mathbb{Z}_2 subgroup. At each of these fixed points the stability matrix has at least one negative eigenvalue, indicating that none of them are stable.

Table 5: Fixed points found for an $O(2)$ bulk.

Symmetry	h^2	h_i^2	$\# \kappa < 0, =0$
\mathbb{Z}_2	1.7163	0.4849	1, 1
\mathbb{Z}_2	2.7224	0.5823	2, 1
\mathbb{Z}_2	3.5613	4.5327	3, 1

For $N = 3$ the situation becomes more complicated, with decoupled theories $I \times I \times I$, $O(2) \times I$, $I \times I \times \text{Free}$, $I \times \text{Free} \times \text{Free}$ and $O(2) \times \text{Free}$ and three interacting bulks one may consider: the $O(3)$ critical model, the cubic critical model with symmetry $B_3 = \mathbb{Z}_2^3 \rtimes S_3$, and the interacting $O(2) \times \mathbb{Z}_2$ biconical model. Let us first consider the situation with fully interacting bulks. Taking the bulk to lie at the $O(3)$ fixed point, the interaction tensor is given by

$$\lambda_{ijkl} = \frac{\varepsilon}{11} (\delta_{ij}\delta_{kl} + \delta_{ik}\delta_{jl} + \delta_{il}\delta_{jk}). \quad (4.15)$$

For $N = 3$ there will be a total of ten beta functions, with numerical searches uncovering the seven fixed points listed in Table 6. Examining the number of $\kappa = 0$ eigenvalues, one sees that three of these fixed points break the bulk $O(3)$ to an $O(2)$ symmetry on the defect, matching the three points found for $N = 3$ in [32]. The remaining four points break the bulk $O(3)$ to a discrete subgroup. We can identify the remaining symmetry at one of these points by noting that they correspond to the S_4 fixed point constructed in section 3.2. For the remaining three fixed points, we attempt to identify the symmetry by explicitly constructing the action of $O(3)$ on the tensor h_{ijk} and identifying the stabiliser of a representative solution. Using the expression for a generic $O(3)$ rotation in terms of three angles,

$$R_{ij} = \begin{pmatrix} \cos \alpha \cos \beta & -\cos \gamma \sin \alpha + \cos \alpha \sin \beta \sin \gamma & \cos \alpha \cos \gamma \sin \beta + \sin \alpha \sin \gamma \\ \sin \alpha \cos \beta & \cos \gamma \cos \alpha + \sin \alpha \sin \beta \sin \gamma & \sin \alpha \cos \gamma \sin \beta - \cos \alpha \sin \gamma \\ -\sin \beta & \cos \beta \sin \gamma & \cos \beta \cos \gamma \end{pmatrix}, \quad (4.16)$$

we numerically solve for α , β and γ satisfying

$$R_{ia}R_{jb}R_{kc}h_{abc} = h_{ijk}. \quad (4.17)$$

For one fixed point, we find that there are six invariant rotations, forming a remaining symmetry group S_3 . While it seems that a \mathbb{Z}_2^2 symmetry remains at the two other points, this is at odds with the existence of pairs of degenerate stability matrix eigenvalues at these points. These pairs of eigenvalues would normally suggest that the symmetry group ought to possess a two-dimensional irreducible representation, which is not the case for \mathbb{Z}_2^2 . It is possible that the degeneracy of these eigenvalues is an accidental one loop effect which will be lifted upon the inclusion of higher order terms in the beta function.

Table 6: Fixed points found for an $O(3)$ bulk.

Symmetry	h^2	h_i^2	$\# \kappa < 0, =0$
$O(2)$	0.9649	0.0491	3, 2
S_4	1.909	0	1, 3
Continued on next page			

Table 6 – continued from previous page

Symmetry	h^2	h_i^2	$\# \kappa < 0, =0$
\mathbb{Z}_2^2	3.574	0.8779	4, 3
\mathbb{Z}_2^2	4.8467	2.1506	5, 3
$O(2)$	5.1972	8.1514	8, 2
$O(2)$	6.0256	3.4477	7, 2
S_3	6.9037	3.1791	6, 3

The essential feature of Table 6 is the variety of symmetry breaking patterns which arise, marking the difference between interface theories, and defects with lower dimension. For the $O(3)$ line defect theory, the only possible defect fixed point retained a continuous $O(2)$ symmetry corresponding to choosing a preferred direction [28]. While the $O(3)$ surface defect possesses one more fixed point than the $O(3)$ line defect, the remaining symmetry groups, $O(3)$ and $O(2) \times \mathbb{Z}_2$ respectively, are both continuous [30]. With the interface, it is possible to break the symmetry generators entirely and gain access to the discrete subgroups of $O(3)$.

Switching now to the critical cubic bulk, the tensor λ_{ijkl} has the form

$$\lambda_{ijkl} = \frac{\varepsilon}{9} (\delta_{ij}\delta_{kl} + \delta_{ik}\delta_{jl} + \delta_{il}\delta_{jk}) - \frac{\varepsilon}{9} \delta_{ijkl}, \quad (4.18)$$

where δ_{ijkl} is the four-index generalisation of the Kronecker delta. We again solve the resulting ten beta functions numerically to find a total of 26 distinct fixed points, shown in Table 7. As the initial bulk symmetry is discrete, breaking is not accompanied by any marginal tilt operators, which is reflected by the lack of $\kappa = 0$ eigenvalues. Of note is the fact that each of the fixed points has at least one $\kappa < 0$ eigenvalue, so that they are all unstable. Two of these points have negative-definite stability matrices, indicating that these will be UV-stable rather than IR-stable fixed points. The stability that remains at a fixed point can be determined in a number of different ways. As the cubic group is of order $8 \times 3! = 48$, the orbit of a fixed point, the set of fixed points with the same values of h^2 and h_i^2 , must be an integer divisor of 48. By the orbit stabiliser theorem, the order of the remaining symmetry group H can thus be determined provided the numerical computations are able to generate the complete orbit. In practice the numerical solver does not seem to be able to generate such complete lists and often the order of the orbit one finds is not a divisor of 48. Instead, we will determine the symmetry by acting explicitly on a representative member of an orbit with the elements of B_3 . As the cubic group is finite, this is easier than in the $O(3)$ case, and we are able to determine precisely which elements preserve the fixed point tensor h_{ijk} . The result is displayed in the first column of Table 7.

Table 7: Fixed points found for a cubic bulk.

Symmetry	h^2	$ h_i ^2$	$\# \kappa < 0, =0$
\mathbb{Z}_2	1.5652	0.1391	5, 0
\mathbb{Z}_2^2	3.153	0.3772	5, 0
\mathbb{Z}_2^2	3.242	1.1784	6, 0
S_3	3.5151	0.2	6, 0
\mathbb{Z}_2	3.8128	1.0632	5, 0
S_3	3.9508	2.7339	6, 0
S_4	4	0	7, 0
\mathbb{Z}_2	4.0567	0.9064	6, 0
\mathbb{Z}_2	4.0649	1.0211	7, 0
None	4.1977	1.8209	6, 0
None	4.3628	1.7113	7, 0
\mathbb{Z}_2	4.3682	1.073	6, 0
\mathbb{Z}_2	4.4154	1.6658	8, 0
\mathbb{Z}_2	4.6101	2.5405	7, 0
S_3	4.7554	2.4035	7, 0
\mathbb{Z}_2^2	4.8298	7.5922	8, 0
\mathbb{Z}_2	5.0071	7.1291	9, 0
S_3	5.022	7.0846	10, 0
\mathbb{Z}_2	5.1195	1.6451	7, 0
\mathbb{Z}_2^2	5.3959	2.9045	8, 0
\mathbb{Z}_2	5.6296	2.6667	7, 0
D_4	5.8115	8.546	10, 0
\mathbb{Z}_2	6.0861	2.7389	8, 0
\mathbb{Z}_2	6.657	3.1942	8, 0
S_3	7.1355	4.7822	9, 0
D_4	7.6863	4.1457	9, 0

One again sees that the symmetry breaking patterns which can appear are more intricate than for other types of defects. While the cubic surface defect has not yet been studied, the cubic line defect was investigated in [28]. Three non-trivial dCFTs were identified, with D_4 , \mathbb{Z}_2^2 and S_4 symmetry corresponding to choosing the privileged vector to lie in the centre of a face, edge or vertex respectively. In Table 7 these symmetry groups are not only joined by the groups \mathbb{Z}_2 and S_3 , but one also sees that there may exist multiple realisations of the same symmetry group.

Rather interestingly, it is also possible for the introduction of the interface to completely break the bulk symmetry, something which was not observed with the line defect.

Let us now consider taking the bulk to lie at the interacting $O(2) \times \mathbb{Z}_2$ biconical critical bulk point. Here, the interaction tensor has irrational coefficients, and it is best expressed by contracting with factors of ϕ_i

$$\lambda_{ijkl}\phi_i\phi_j\phi_k\phi_l = 0.252845(\phi_1^2 + \phi_2^2)^2 + 0.690589(\phi_1^2 + \phi_2^2)\phi_3^2 + 0.20248\phi_3^4. \quad (4.19)$$

Solving the beta functions numerically we find a total of nine fixed points, displayed in Table 8. As may be expected from the irrational bulk couplings, all of the fixed points have irrational invariants. The single $\kappa = 0$ eigenvalue at each fixed point indicates that in all cases the bulk $O(2)$ symmetry is broken by the defect to a discrete subgroup. As before, we determine the remaining symmetry by explicitly constructing the action of $O(2) \times \mathbb{Z}_2$ on a representative solution from each equivalency class. The result is displayed in the first column of Table 8. It is also worth noting that as for the other two bulks, each fixed point possesses at least one relevant operator, and is thus unstable.

Table 8: Fixed points found for an $O(2) \times \mathbb{Z}_2$ biconical bulk.

Symmetry	h^2	$ h_i ^2$	$\# \kappa < 0, =0$
\mathbb{Z}_2^2	0.12418	0.00220839	2, 1
\mathbb{Z}_2^2	0.143199	0.00306045	3, 1
\mathbb{Z}_2^2	1.43105	0.0813986	4, 1
\mathbb{Z}_2	2.45154	0.245134	4, 1
D_4	3.09495	0	6, 1
\mathbb{Z}_2	3.53387	1.30149	5, 1
\mathbb{Z}_2^2	5.40366	8.28185	9, 1
\mathbb{Z}_2^2	6.66652	3.59745	8, 1
\mathbb{Z}_2^2	7.93982	0.279441	5, 1

We display the results of Tables 6-8 graphically in Fig. 4, plotting the values of the $O(3)$ invariants h_i^2 versus h^2 . As these three bulks are the only possible fully interacting critical points for three scalar fields, this set of fixed points will be a complete classification of interface dCFTs with three scalars in a critical interacting bulk theory. It is interesting to note that the fixed points of the various bulk models occupy similar regions of this space of invariants, perhaps suggesting that the form of the fixed point solutions are related.

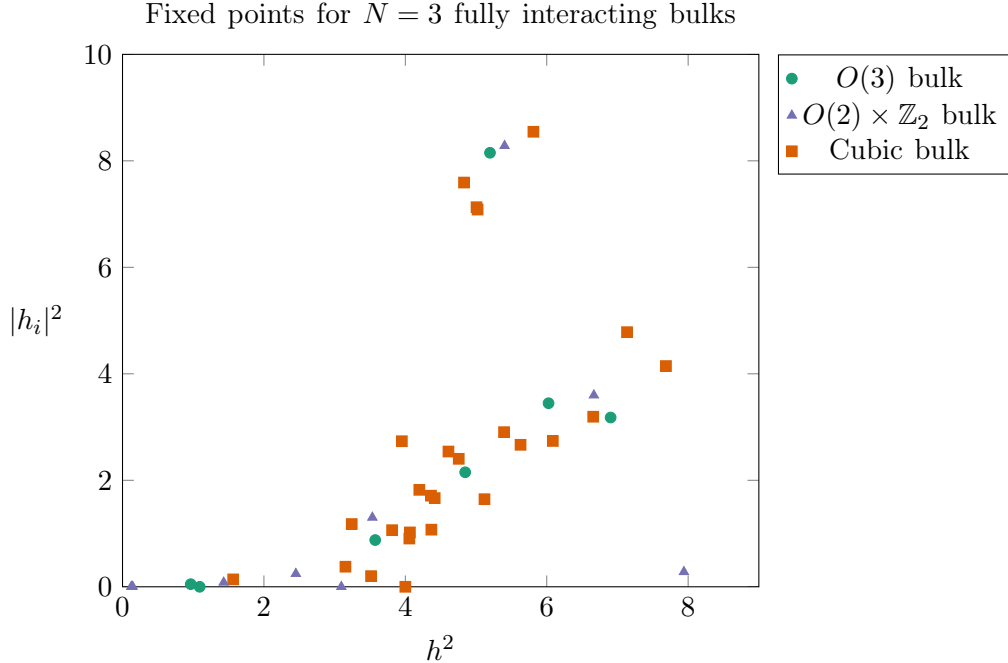


Fig. 4: Unitary fixed points for $N = 3$ interacting bulks found using a numerical search beginning with 10,000 points. We find 7 fixed points in an $O(3)$ bulk, 26 in a cubic bulk, and 9 in an $O(2) \times \mathbb{Z}_2$ biconical bulk. Not shown is the trivial fixed point $h_{ijk} = 0$, which is the only stable point for all three bulks.

We can now turn to decoupled bulk models. While one could restrict one's attention to deforming only by operators which do not combine fields not already coupled in the bulk, it is more interesting to consider fixed points which cause the bulk fields to become interacting on the defect. Let us first consider the bulk to lie at an $O(2)$ point for the fields ϕ_1 and ϕ_2 , while the field ϕ_3 is left free, giving the bulk a symmetry group of $O(2) \times \mathbb{Z}_2$. To be precise, the interaction tensor will take the form

$$\lambda_{ijkl}\phi_i\phi_j\phi_k\phi_l = \frac{3\varepsilon}{10}(\phi_1^2 + \phi_2^2)^2, \quad (4.20)$$

where unlike (4.12) i, j, k, l run from 1 to 3. The numerical results are displayed in Table 9. As there exist no non-trivial fixed points for the $N = 1$ free bulk, we find only the three decoupled fixed points deriving from Table 5. The remaining three fixed points cause ϕ_3 to non-trivially interact with ϕ_1 and ϕ_2 along the interface. One of these points retains the $O(2)$ rotational symmetry of ϕ_1 and ϕ_2 , while the other two completely break the bulk symmetry group.

Table 9: Fixed points found for an $O(2) \times \text{Free}$ bulk.

Symmetry	h^2	$ h_i ^2$	$\# \kappa < 0, =0$
\mathbb{Z}_2^2	1.7163	0.4849	6, 1
Continued on next page			

Table 9 – continued from previous page

Symmetry	h^2	$ h_i ^2$	$\# \kappa < 0, =0$
\mathbb{Z}_2^2	2.7224	0.5823	7, 1
\mathbb{Z}_2^2	3.5613	4.5327	8, 1
$O(2)$	25.7941	2.8091	7, 0
None	27.2925	3.4681	7, 1
None	27.6885	3.6268	8, 1

We can also take the bulk to be the direct sum of an $O(2)$ theory and an Ising theory. Here, the interaction tensor may be expressed as

$$\lambda_{ijkl}\phi_i\phi_j\phi_k\phi_l = \frac{3\varepsilon}{10}(\phi_1^2 + \phi_2^2)^2 + \frac{\varepsilon}{3}\phi_3^4, \quad (4.21)$$

which differs from (4.19) in the lack of a term mixing ϕ_3 with ϕ_1 and ϕ_2 . Solving the beta functions numerically, we find that, unlike for the decoupled $I \times I$ theory, direct sums of $O(2)$ solutions with \mathbb{Z}_2 solutions are not the only possible fixed points. In the end a total of 12 fixed points appear, as displayed in Table 8. Seven of these correspond to decoupled fixed points, whose symmetry may be easily determined from the form of the potential. The remaining five are theories in which the ϕ_3 field, decoupled in the bulk, is able to interact along the interface with the other two fields ϕ_1 and ϕ_2 . Examining the $\kappa = 0$ eigenvalues, one sees that one of these extra points preserves the $O(2)$ symmetry of the ϕ_1 and ϕ_2 fields. To determine the remaining symmetry at the other fixed points we once again construct the action of $O(2)$ on the fields, and determine that no symmetry remains.

Table 10: Fixed points found for a decoupled $O(2) \times I$ bulk.

Symmetry	h^2	$ h_i ^2$	$\# \kappa < 0, =0$
\mathbb{Z}_2^2	1.7163	0.4849	6, 1
$O(2)$	2	2	6, 0
\mathbb{Z}_2^2	2.7224	0.5823	7, 1
$O(2)$	2.9215	0.4738	7, 0
\mathbb{Z}_2^2	3.5613	4.5327	8, 1
\mathbb{Z}_2	3.7163	2.4849	7, 1
\mathbb{Z}_2	4.7224	2.5823	8, 1
\mathbb{Z}_2	5.5613	6.5327	9, 1
None	7.2701	1.8644	7, 1
Continued on next page			

Table 10 – continued from previous page

Symmetry	h^2	$ h_i ^2$	$\# \kappa < 0, =0$
None	7.5703	1.9352	7, 1
None	9.4071	1.7039	8, 1
None	9.9475	2.6177	8, 1

Let us now consider a bulk which is taken to be the direct sum of three decoupled Ising fixed points. The interaction tensor in this case will be

$$\lambda_{ijkl}\phi_i\phi_j\phi_k\phi_l = \frac{\varepsilon}{3}(\phi_1^4 + \phi_2^4 + \phi_3^4), \quad (4.22)$$

which is invariant under the cubic group $B_3 = \mathbb{Z}_2^3 \rtimes S_3$. There exists a fictitious conformal manifold in this model, given explicitly by the deformation

$$3h\phi_1^2\phi_3 + \frac{2}{h}\phi_2^2\phi_3 - \frac{2+3h^2}{3h}\phi_3^3. \quad (4.23)$$

One can check that these fixed points do not survive at two loops, and should thus be ignored in a complete classification. Noting that these fixed points have the same $O(N)$ invariant $h_i^2 = 0$ for all values of h , in the numerical search we allow only fixed points with $h_i^2 \neq 0$. While it is possible that there exist other, genuine fixed points with vanishing h_i^2 , we note that in other decoupled bulks all fixed points obey $h_i^2 \neq 0$, so that we believe that our numerical search will still be exhaustive. In the end, the numerical search reveals the eight fixed points shown in Table 11. As the bulk symmetry group is finite, it is possible to explicitly construct the broken generators to determine the remaining symmetry at these fixed points, as in the case of the cubic fixed point.

Table 11: Fixed points found for a decoupled $I \times I \times I$ bulk.

Symmetry	h^2	$ h_i ^2$	$\# \kappa < 0, =0$
\mathbb{Z}_2^3	2	2	8, 0
\mathbb{Z}_2^2	4	4	9, 0
S_3	6	6	10, 0
\mathbb{Z}_2	11.8304	0.9834	8, 0
\mathbb{Z}_2	13.4965	1.6436	7, 0
S_3	17.1538	3.0936	9, 0
\mathbb{Z}_2	20.2542	2.0717	8, 0
\mathbb{Z}_2^2	25.3646	0.4005	8, 0

Removing the ϕ_3^4 term, we arrive at a bulk with two fields at the Ising point and one free field,

$$\lambda_{ijkl}\phi_i\phi_j\phi_k\phi_l = \frac{\varepsilon}{3}(\phi_1^4 + \phi_2^4), \quad (4.24)$$

with a bulk symmetry group $(\mathbb{Z}_2^2 \times \mathbb{Z}_2) \times \mathbb{Z}_2$. The numerics produce the five fixed points in Table 12, where once again because the symmetry group is finite we are able to explicitly determine the number of broken generators at each fixed point. Two of these points correspond to decoupled direct sums of the Ising interface with a free ϕ_3 , but the remaining points non-trivially couple the three fields.

Table 12: Fixed points found for an $I \times I \times \text{Free}$ bulk.

Symmetry	h^2	$ h_i ^2$	$\# \kappa < 0, =0$
\mathbb{Z}_2^2	2	2	9, 0
\mathbb{Z}_2^2	4	4	10, 0
\mathbb{Z}_2	33.5888	3.4233	7, 0
$\mathbb{Z}_2^2 \times \mathbb{Z}_2$	33.5912	3.3578	7, 0
\mathbb{Z}_2	34.7502	3.7924	8, 0

Finally, we can take two of the bulk fields to be free, and the remaining field, which we choose to be ϕ_1 to lie at the Ising critical point,

$$\lambda_{ijkl}\phi_i\phi_j\phi_k\phi_l = \frac{\varepsilon}{3}\phi_1^4. \quad (4.25)$$

This will have a bulk symmetry group $G = O(2) \times \mathbb{Z}_2$. We again find five fixed points, exhibited in Table 13. The first of these points is decoupled, but the remaining four are fully interacting fixed points.

Table 13: Fixed points found for an $I \times \text{Free} \times \text{Free}$ bulk.

Symmetry	h^2	$ h_i ^2$	$\# \kappa < 0, =0$
$O(2)$	2	2	10, 0
$O(2)$	44.3429	2.3688	9, 0
None	53.0497	4.5056	7, 1
\mathbb{Z}_2	53.0504	4.4683	7, 1
None	54.1261	4.7865	8, 1

We display the results of Table 1 and Tables 10-13 in Fig. 5. Comparing with Fig. 4 one notices immediately that while the decoupled bulks can have considerably larger values of h^2 , all fixed points seem to obey a bound of the form $|h_i|^2 \lesssim 9$. As we have considered all possible bulks for $N \leq 3$, the fixed points we have identified should provide a complete classification of scalar interface dCFTs with three or fewer fields.

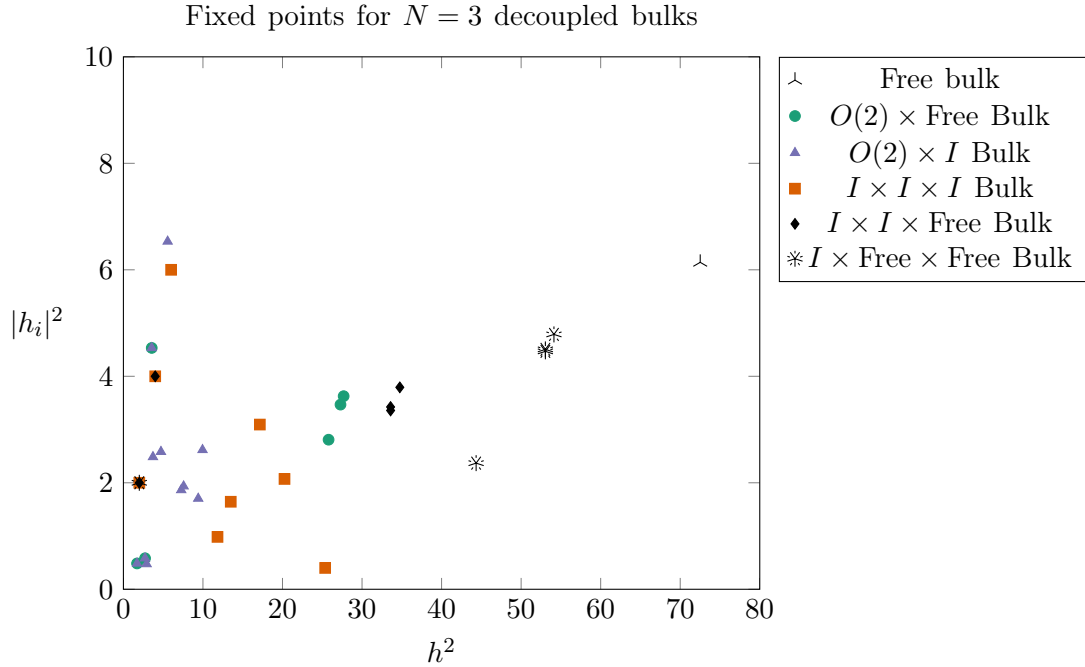


Fig. 5: Unitary fixed points for $N = 3$ decoupled bulks found using a numerical search beginning with 10,000 points. The fixed points can also be found in Table 1 and Tables 9-13.

4.2. Larger numbers of fields

For larger numbers of fields the number of possible critical bulk models one can choose from grows rapidly, and we will thus focus only on placing interfaces within well-known models. As our bulk models we choose the free bulk, the $O(N)$ model, the hypercubic $B_N = \mathbb{Z}_2^N \rtimes S_N$ model and the two hypertetrahedral $T_N^\pm = S_{N+1} \times \mathbb{Z}_2$ models, which have applications in a variety of physical systems. The number of fixed points we find numerically grows rapidly with N , as indicated by Table 14. Here we have used a number of small N isomorphisms between bulk fixed points and results from Tables 1-13 to include results for hypercubic and hypertetrahedral models even for N

Table 14: Number of fixed points found for various N

Bulk Model	$N = 1$	$N = 2$	$N = 3$	$N = 4$	$N = 5$	$N = 6$	$N = 7$	$N = 8$
Free	0	0	1	5	18	48	136	71
$O(N)$	1	3	7	N/A	14	35	159	50
B_N	1	2	26	N/A	883	616	293	16
T_N^-	1	3	26	169	1671	1560	395	28
T_N^+	1	0	8	N/A	1671	1584	350	23

in which they were not explicitly considered. N/A indicates the presence of a leading-order conformal manifold, like the one discussed at the end of section 3.2, which prevented the numerics from providing accurate results. Though the number of fixed points found decreases sharply for the larger N we looked at, we suspect that this is a numerical artefact associated with *Mathematica* facing difficulty working within a high-dimensional solution space. All of the numerical results were derived beginning with 10,000 initial points, and it is likely that at higher N this is not sufficient to provide a satisfactory search of coupling space. Our numerical results stop at $N = 8$, where there are already 120 equations and unknowns, as beyond this point the `FindRoot` function becomes prohibitively slow.

We display the results of our numerical searches for $4 \leq N \leq 8$ in Fig. 6-10. The appearance of a leading-order conformal manifold of fixed points for the $O(4)$ and B_4 models inhibits our numerical searches, so these models are omitted from Fig. 6. It is important to note that none of the identified fixed points, ignoring the trivial fixed point, were stable against generic deformations. Of interest is the fact that the value of the h_i^2 invariant appears to be bounded from above for all of the interacting bulk theories, though we were unable to find an analytic form for such a bound. In all of the examined cases we find a rich zoo of symmetry breaking patterns. For the $O(N)$ models and free bulks the number of $\kappa = 0$ eigenvalues gives an indication of the continuous symmetry group remains, though it does not allow us to determine if there are additional discrete group factors. We find that beyond the breaking to $O(N - 1)$ studied previously, there are multiple breakings to smaller orthogonal groups in addition to a sea of fixed points with only discrete symmetry remaining. For the hypercubic and hypertetrahedral models it is possible to estimate the order of the symmetry group remaining at a fixed point using the number of physically equivalent theories. As the numerics inevitably do not find all of the fixed points in every orbit, this is an imperfect process, but indicates that for these groups, too, the space of interface dCFTs is rich in potential symmetry breaking patterns.

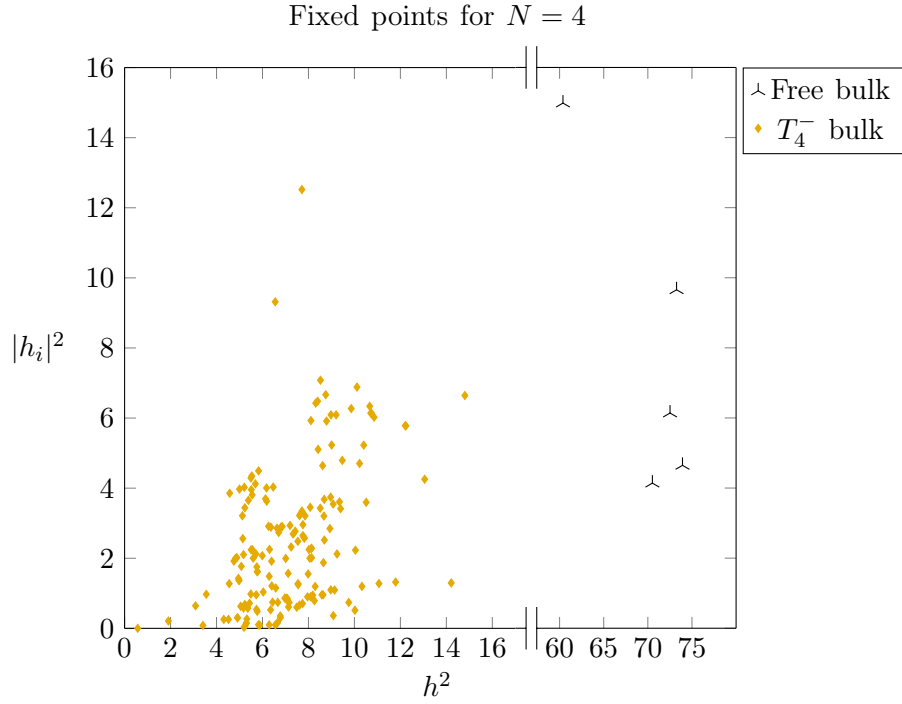


Fig. 6: Unitary fixed points for $N = 4$ found using a numerical search beginning with 10,000 points.

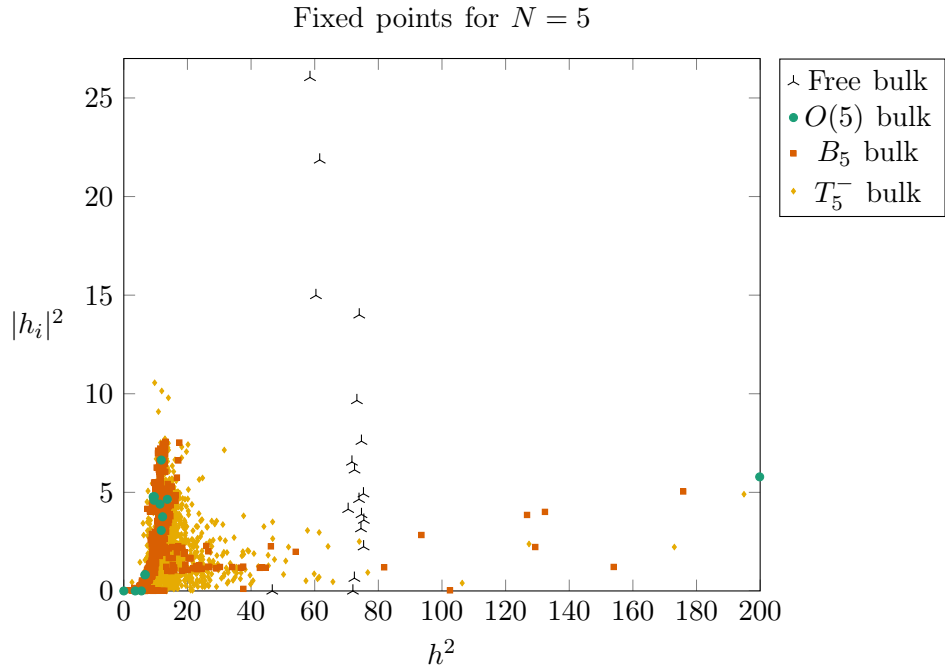


Fig. 7: Unitary fixed points for $N = 5$ found using a numerical search beginning with 10,000 points.

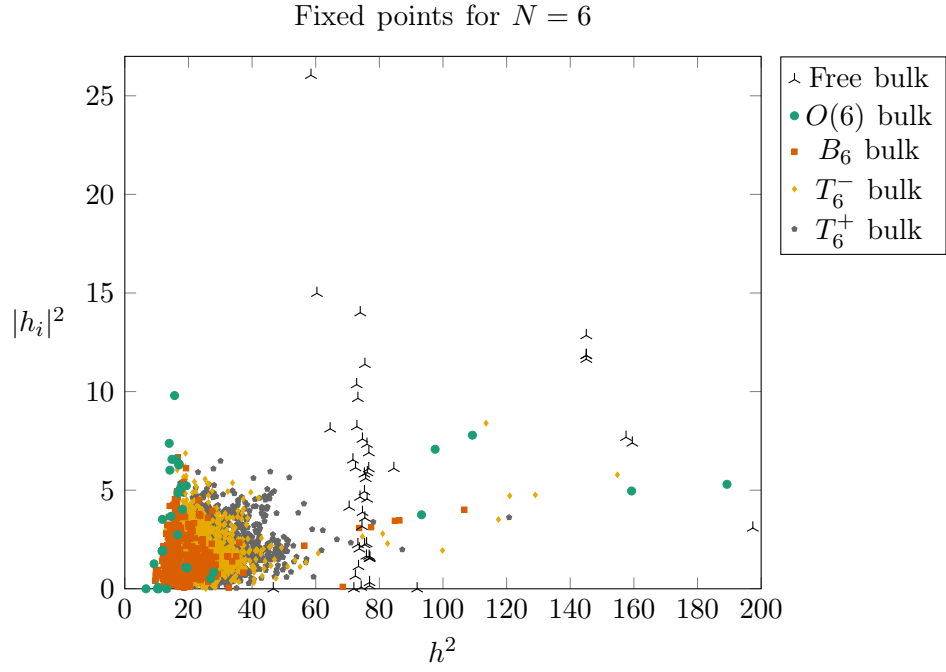


Fig. 8: Unitary fixed points for $N = 6$ found using a numerical search beginning with 10,000 points.

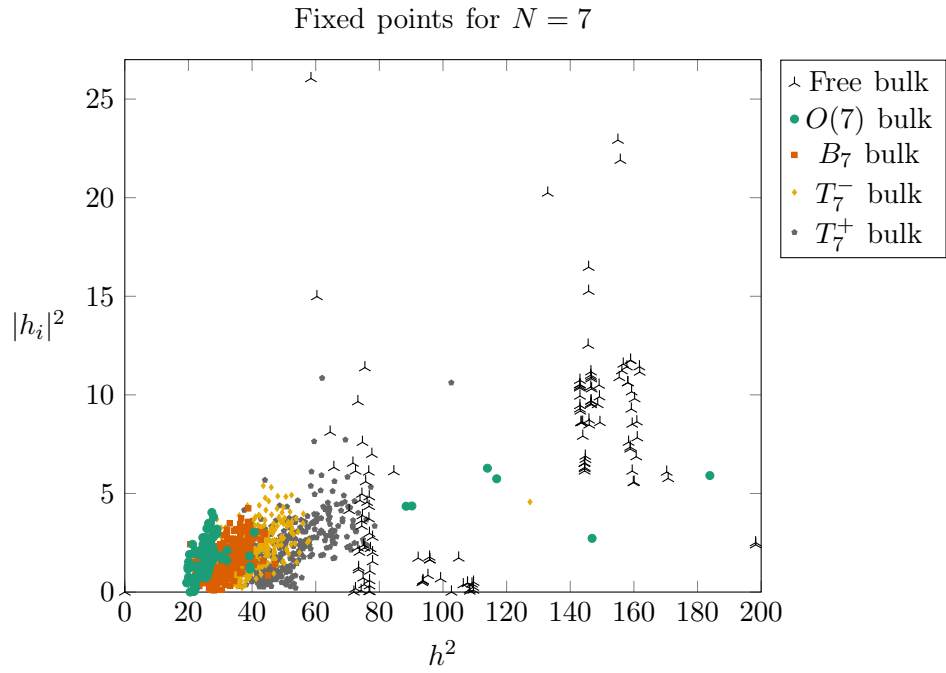


Fig. 9: Unitary fixed points for $N = 7$ found using a numerical search beginning with 10,000 points.

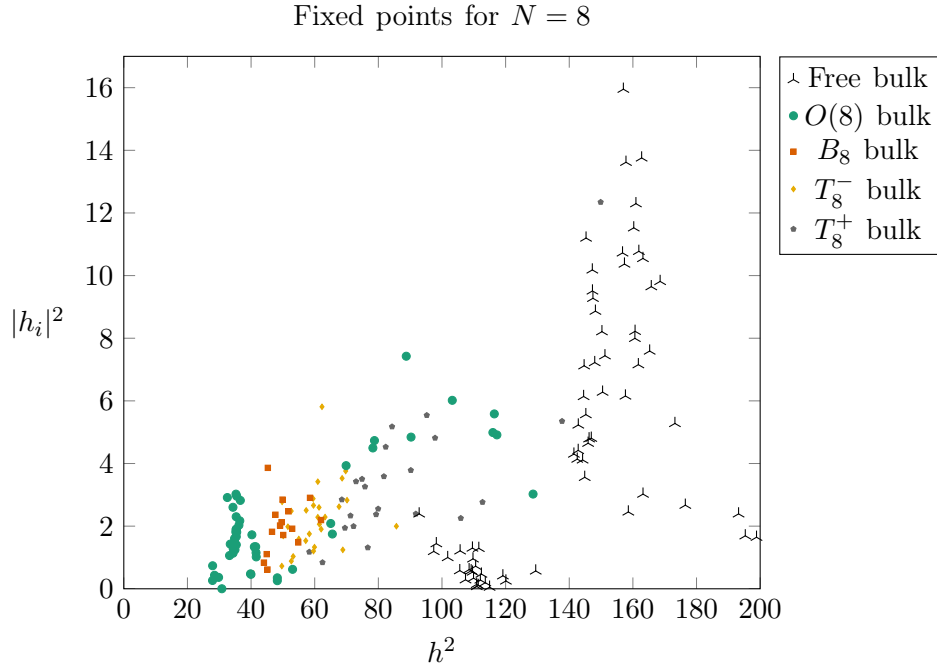


Fig. 10: Unitary fixed points for $N = 8$ found using a numerical search beginning with 10,000 points.

5. Conclusion

In this work we studied the space of interface CFTs that arise when well-known CFTs in $4 - \varepsilon$ dimensions are perturbed by localised interactions cubic in ϕ . Our results indicate that this is an extensive space, comprising interface fixed points with global symmetries given by subgroups of the global symmetry of the bulk CFT in which they live. In many instances we find multiple interface CFTs with the same global symmetry, and we also find interface CFTs with no global symmetry whatsoever. The interface CFTs we have found always have at least one relevant operator. We have focused on unitary theories, but our methods are also applicable to non-unitary ones, which typically include fixed points that are RG stable as was already noticed in [32].

The study of fixed points within the framework of the perturbative ε expansion is valuable, as it reveals aspects of the space of CFTs that can guide research with non-perturbative methods, e.g. the conformal bootstrap. While we have resorted to a standard perturbative treatment, analytic bootstrap methods can also be used to study the spectrum and operator product expansion coefficients of interface CFTs, as already discussed in [40]. Of course our results here are strictly valid for ε small, and their continuation to $\varepsilon = 1$ is not obvious. Nevertheless, our results indicate that the space of two-dimensional interface CFTs that live in three-dimensional space is vast. Perhaps it can be charted by applying the bootstrap methods of [41] or extending those of [42, 43] to interfaces or by applying the folding trick. The theories with $SO(3)$, $SU(3)$, $Sp(6)$ and F_4 global

symmetries discussed in this work would offer obvious targets.

Further possible extensions of this work include the consideration of surface defects in bulk universality classes beyond the $O(N)$ model, as has been done here for interfaces and in [28] for line defects. Composite defects [44], where the combined effects of an interface hosting a lower-dimensional defect can also be studied with the ε expansion. This would presumably give rise to new universality classes that have not yet been explored. Multiple interfaces and the effective field theory that may be defined for them can also be analysed, using the framework recently discussed in [45, 46]. Finally, the analysis of interfaces that separate two different CFTs in the ε expansion would offer a variety of avenues for investigation.

Acknowledgments

We would like to thank Hugh Osborn for insightful comments that led to our discussion of the F_4 family of fixed points. The numerical computations in this work have used King’s College London’s CREATE [47] computing resources. Some computations in this paper have been performed with the help of *Mathematica* with the packages `xAct` [48] and `xTras` [49]. Nordita is supported in part by NordForsk. AS is supported by the Royal Society under grant URF\R1\211417 and by STFC under grant ST/X000753/1. AS thanks the CERN Department of Theoretical Physics for hospitality during the final stages of completion of this work.

Appendix A. Preliminary two-loop results

In this appendix we gather results on the computation of the two-loop interface beta function.

The beta function of the bulk coupling is not affected by the interface and is given by

$$\begin{aligned} \beta_{ijkl} = & -\varepsilon\lambda_{ijkl} + (\lambda_{ijmn}\lambda_{mnkl} + 2 \text{ perms}) - (\lambda_{ijmn}\lambda_{mefk}\lambda_{nefl} + 5 \text{ perms}) \\ & + \frac{1}{12}(\lambda_{ijkm}\lambda_{mnef}\lambda_{nefl} + 3 \text{ perms}). \end{aligned} \tag{A.1}$$

At two loops, three type of graphs contribute to the three-point function on the interface: one-particle-irreducible graphs with only cubic couplings, one-particle-irreducible graphs with both cubic and quartic couplings and one-particle-reducible graphs coming from corrections to the two-point function. They are represented in Fig. 1, 2 and 3 respectively.

With the notation of (2.9), the three-point function at two loops is given by

$$\begin{aligned}
\mu^{-2\varepsilon} \mathcal{A}_{ijk}^{(2)} = & (h_{ide} h_{dfg} h_{efl} h_{jgm} h_{klm} + 2 \text{ perms}) I_1 + (h_{ide} h_{jdf} h_{kgf} h_{glm} h_{elm} + 2 \text{ perms}) I_2 \\
& + h_{ide} h_{jfg} h_{klm} h_{dfl} h_{egm} I_3 + (\lambda_{ijef} \lambda_{efgl} h_{glk} + 2 \text{ perms}) B_2 \\
& + (\lambda_{idef} \lambda_{jdel} h_{flk} + 2 \text{ perms}) S_1 + (\lambda_{ijef} \lambda_{eglk} h_{glf} + 2 \text{ perms}) S_2, \\
& + (\lambda_{iefg} h_{efl} h_{lmj} h_{gmk} + 5 \text{ perms}) U_1 + (\lambda_{ijef} h_{egl} h_{fgm} h_{mlk} + 2 \text{ perms}) U_2 \\
& + (\lambda_{efgl} h_{ief} h_{jgm} h_{klm} + 2 \text{ perms}) U_3 + (\lambda_{ijde} h_{kdf} h_{fml} h_{eml} + 2 \text{ perms}) U_4 \\
& + (\lambda_{kdml} h_{ide} h_{jfl} h_{efm} + 2 \text{ perms}) U_5 + (\lambda_{efgl} \lambda_{kfgl} h_{ije} + 2 \text{ perms}) M \\
& + (h_{ije} h_{efg} h_{lmk} \lambda_{fglm} + 2 \text{ perms}) K_1 + (h_{ije} h_{fgl} h_{glm} \lambda_{efmk} + 2 \text{ perms}) K_2 \\
& + (h_{ije} h_{efg} h_{flm} \lambda_{lmgk} + 2 \text{ perms}) K_3 + (h_{ije} h_{lmg} h_{gfk} \lambda_{elmf} + 2 \text{ perms}) K_4. \quad (\text{A.2})
\end{aligned}$$

We now need to compute the counterterms needed to make the three-point function finite. They can be obtained directly for each graph by using the Bogoliubov-Parasuk recursion formula [50]. We will then project onto the simple poles in $1/\varepsilon$ to obtain the beta function coefficients.

Denoting

$$\begin{aligned}
Z_{ijk}^{(1)} = & a_T h_{ide} h_{jdf} h_{kef} + a_{I_1} (h_{ide} h_{dfg} h_{efl} h_{jgm} h_{klm} + 2 \text{ perms}) \\
& + a_{I_2} (h_{ide} h_{jdf} h_{kgf} h_{glm} h_{elm} + 2 \text{ perms}) + a_{I_3} h_{ide} h_{jfg} h_{klm} h_{dfl} h_{egm} \\
& + a_B (\lambda_{ijef} h_{efk} + 2 \text{ perms}) + a_{B_2} (\lambda_{ijef} \lambda_{efgl} h_{glk} + 2 \text{ perms}) \\
& + a_{S_1} (\lambda_{idef} \lambda_{jdel} h_{flk} + 2 \text{ perms}) + a_{S_2} (\lambda_{ijef} \lambda_{eglk} h_{glf} + 2 \text{ perms}), \\
& + a_{U_1} (\lambda_{iefg} h_{efl} h_{lmj} h_{gmk} + 5 \text{ perms}) + a_{U_2} (\lambda_{ijef} h_{egl} h_{fgm} h_{mlk} + 2 \text{ perms}) \\
& + a_{U_3} (\lambda_{efgl} h_{ief} h_{jgm} h_{klm} + 2 \text{ perms}) + a_{U_4} (\lambda_{ijde} h_{kdf} h_{fml} h_{eml} + 2 \text{ perms}) \\
& + a_{U_5} (\lambda_{kdml} h_{ide} h_{jfl} h_{efm} + 2 \text{ perms}) + a_M (\lambda_{efgl} \lambda_{kfgl} h_{ije} + 2 \text{ perms}) \\
& + a_{K_1} (h_{ije} h_{efg} h_{lmk} \lambda_{fglm} + 2 \text{ perms}) + a_{K_2} (h_{ije} h_{fgl} h_{glm} \lambda_{efmk} + 2 \text{ perms}) \\
& + a_{K_3} (h_{ije} h_{efg} h_{flm} \lambda_{lmgk} + 2 \text{ perms}) + a_{K_4} (h_{ije} h_{lmg} h_{gfk} \lambda_{elmf} + 2 \text{ perms}), \quad (\text{A.3})
\end{aligned}$$

we have

$$\begin{aligned}
a_T &= -(2\pi)^2 T^{(1)}, & a_{I_1} &= (2\pi)^4 (-I_1^{(1)} + T^{(1)}T^{(0)}), \\
a_{I_2} &= -(2\pi)^4 I_2^{(1)}, & a_{I_3} &= -(2\pi)^4 I_3^{(1)}, \\
a_B &= -(4\pi)^2 B^{(1)}, & a_{S_1} &= (4\pi)^4 (2B^{(0)}D^{(1)} - S_1^{(1)}) \\
a_{S_2} &= (4\pi)^4 (2B^{(0)}B^{(1)} - S_2^{(1)}), & a_{B_2} &= (4\pi)^4 (B^{(0)}B^{(1)} + B^{(0)}D^{(1)} - B_2^{(1)}), \\
a_{U_1} &= 4(2\pi)^4 (B^{(1)}T^{(0)} - U_1^{(1)}), & a_{U_2} &= 4(2\pi)^4 (B^{(0)}T^{(1)} - U_2^{(1)}), \\
a_{U_3} &= 4(2\pi)^4 (B^{(1)}T^{(0)} - U_3^{(1)}), & a_{U_4} &= -4(2\pi)^4 U_4^{(1)}, \\
a_{U_5} &= -4(2\pi)^4 U_5^{(1)}, & a_{K_1} &= -4(2\pi)^4 K_1^{(1)}, \\
a_{K_2} &= -4(2\pi)^4 K_2^{(1)}, & a_{K_3} &= a_{K_4} = -4(2\pi)^4 K_3^{(1)}, \\
a_M &= -(4\pi)^4 \left(M^{(1)} + \frac{1}{24} \right), & &
\end{aligned} \tag{A.4}$$

where we have parameterised the amplitude of a ℓ -loop graph \mathcal{G} as $\mathcal{A}(\mathcal{G}) = \mu^{-\ell\varepsilon} \sum_{k=0}^{\ell} \frac{\mathcal{G}^{(k)}}{\varepsilon^k}$. D is the amplitude of the bulk one-loop bubble graph with two quartic couplings contributing to the renormalisation of the bulk coupling

$$D = \text{bubble diagram} = -\frac{\mu^{-\varepsilon}}{16\pi^2\varepsilon} + \mathcal{O}(\varepsilon^0). \tag{A.5}$$

The counterterm in the coefficient a_M comes from the one-loop part of the bulk wavefunction renormalisation factor (2.4).

Using (2.14), we finally obtain the two-loop beta functions of the interface coupling

$$\begin{aligned}
\beta_{ijk} &= -\frac{\varepsilon}{2} h_{ijk} + a_T h_{ide} h_{jdf} h_{kef} + 2a_{I_1} (h_{ide} h_{dfg} h_{efl} h_{jgm} h_{klm} + 2 \text{ perms}) \\
&+ 2a_{I_2} (h_{ide} h_{jdf} h_{kgf} h_{glm} h_{elm} + 2 \text{ perms}) + 2a_{I_3} h_{ide} h_{jfg} h_{klm} h_{dfl} h_{egm} \\
&+ a_B (\lambda_{ijef} h_{efk} + 2 \text{ perms}) + 2a_{B_2} (\lambda_{ijef} \lambda_{efgl} h_{glk} + 2 \text{ perms}) \\
&+ 2a_{S_1} (\lambda_{idef} \lambda_{jdel} h_{flk} + 2 \text{ perms}) + 2a_{S_2} (\lambda_{ijef} \lambda_{eglk} h_{glf} + 2 \text{ perms}), \\
&+ 2a_{U_1} (\lambda_{iefg} h_{efl} h_{lmj} h_{gmk} + 5 \text{ perms}) + 2a_{U_2} (\lambda_{ijef} h_{egl} h_{fgm} h_{mlk} + 2 \text{ perms}) \\
&+ 2a_{U_3} (\lambda_{efgl} h_{ief} h_{jgm} h_{klm} + 2 \text{ perms}) + 2a_{U_4} (\lambda_{ijde} h_{kdf} h_{fml} h_{eml} + 2 \text{ perms}) \\
&+ 2a_{U_5} (\lambda_{kdml} h_{ide} h_{jfl} h_{efm} + 2 \text{ perms}) + 2a_M (\lambda_{efgl} \lambda_{kfgl} h_{ije} + 2 \text{ perms}) \\
&+ 2a_{K_1} (h_{ije} h_{efg} h_{lmk} \lambda_{fglm} + 2 \text{ perms}) + 2a_{K_2} (h_{ije} h_{fgl} h_{glm} \lambda_{efmk} + 2 \text{ perms}) \\
&+ 2a_{K_3} (h_{ije} h_{efg} h_{flm} \lambda_{lmgk} + 2 \text{ perms}) + 2a_{K_4} (h_{ije} h_{lmg} h_{gfk} \lambda_{elmf} + 2 \text{ perms}). \tag{A.6}
\end{aligned}$$

The amplitudes of the pure interface graphs can be computed and our results were cross-checked with the long-range computation of [51]. The computation of the mixed graphs is more

challenging due to the interface-to-bulk propagator and we were not able to compute all the beta function coefficients. We have

$$\begin{aligned}
a_T &= -\frac{1}{4}, & a_B &= 1, \\
2a_{I_1} &= -\frac{1}{16}, & 2a_{I_2} &= \frac{1}{64}, & 2a_{I_3} &= -\frac{\pi^2}{128}, \\
2a_{B_2} &= 0, & 2a_{S_1} &= -1, & 2a_{S_2} &= -1, \\
2a_{U_2} &= \frac{1}{4}, & 2a_{U_3} &= 0, & 2a_{U_4} &= -\frac{1}{8}, \\
2a_{K_2} &= \frac{1}{16}, & 2a_M &= \frac{1}{12}.
\end{aligned} \tag{A.7}$$

We still have to compute $a_{U_1}, a_{U_5}, a_{K_1}$ and a_{K_3} . In the next subsection we give more details on the computation of the bulk-defect integrals that we have computed so far.

A.1. Computation of bulk-defect integrals

To compute the amplitudes of the graphs contributing to the three-point function we will use repeatedly the following two formulas

$$\int \frac{d^d \mathbf{q}}{(2\pi)^d} \frac{1}{|\mathbf{q}|^{2\alpha} |\mathbf{q} + \mathbf{p}|^{2\beta}} = \frac{|\mathbf{p}|^{d-2\alpha-2\beta}}{(4\pi)^{d/2}} \frac{\Gamma(\frac{d}{2} - \alpha)\Gamma(\frac{d}{2} - \beta)\Gamma(\alpha + \beta - \frac{d}{2})}{\Gamma(\alpha)\Gamma(\beta)\Gamma(d - \alpha - \beta)}, \tag{A.8}$$

and

$$\int \frac{d^d \mathbf{q}}{(2\pi)^d} \frac{1}{|\mathbf{q}|^a (|\mathbf{q}| + |\mathbf{p}|)} = \frac{2|\mathbf{p}|^{d-1-a}}{\Gamma(\frac{d}{2})(4\pi)^{d/2}} \Gamma(d-a)\Gamma(1-d+a). \tag{A.9}$$

A.1.1. Graphs with only one interface coupling

To compute these integrals we use the trick explained at the end of section 2. We obtain

$$2a_{S_1} = 2a_{S_2} = -1, \quad 2a_{B_2} = 0, \quad 2a_M = \frac{1}{12}. \tag{A.10}$$

We were able to compute independently the amplitude B_2 , providing a cross-check of this method.

We have

$$\begin{aligned}
B_2 &= \frac{1}{64} \int \frac{d^d \mathbf{q}_1 d^d \mathbf{q}_2}{(2\pi)^{2d}} \int dy \int dz \frac{e^{-2|\mathbf{q}_1||z|} e^{-2|\mathbf{q}_2||z-y|} e^{-2|\mathbf{p}||y|}}{|\mathbf{q}_1|^2 |\mathbf{q}_2|^2} \\
&= \frac{1}{64} \int \frac{d^d \mathbf{q}_1 d^d \mathbf{q}_2}{(2\pi)^{2d}} \frac{1}{|\mathbf{q}_1|^2 |\mathbf{q}_2|^2} \int dz e^{-2|\mathbf{q}_1||z|} \frac{|\mathbf{q}_2| e^{-2|\mathbf{p}||z|} - |\mathbf{p}| e^{-2|\mathbf{q}_2||z|}}{(|\mathbf{q}_2| + |\mathbf{p}|)(|\mathbf{q}_2| - |\mathbf{p}|)} \\
&= \frac{1}{64} \int \frac{d^d \mathbf{q}_1 d^d \mathbf{q}_2}{(2\pi)^{2d}} \frac{1}{|\mathbf{q}_1|^2 |\mathbf{q}_2|^2 (|\mathbf{q}_2| + |\mathbf{p}|)(|\mathbf{q}_2| - |\mathbf{p}|)} \left(\frac{|\mathbf{q}_2|}{|\mathbf{p}| + |\mathbf{q}_1|} - \frac{|\mathbf{p}|}{|\mathbf{q}_1| + |\mathbf{q}_2|} \right). \tag{A.11}
\end{aligned}$$

It is then possible to integrate over \mathbf{q}_1 using (A.9) to obtain

$$\begin{aligned}
B_2 &= \frac{\mu^{-2\varepsilon}}{16\Gamma^2(\frac{d}{2})(4\pi)^d} \Gamma(d-2)\Gamma(3-d) \int dq \frac{q^{d-2} - q^{2d-6}}{(q+1)(q-1)} \\
&= -\frac{\mu^{-2\varepsilon}}{32\Gamma(\frac{d}{2})^2(4\pi)^d} \Gamma(d-2)\Gamma(3-d) \frac{\pi \tan(\frac{\pi d}{2})}{\cos(\pi d)} \\
&= \frac{\mu^{-2\varepsilon}}{256\pi^4} \left(\frac{1}{\varepsilon^2} + \frac{2-\gamma+\ln\pi}{\varepsilon} + \mathcal{O}(\varepsilon^0) \right). \tag{A.12}
\end{aligned}$$

Using (A.4), we then indeed obtain $a_{B_2} = 0$.

A.1.2. Graphs with more than one interface coupling

The integral U_2 We have

$$\begin{aligned}
U_2 &= -\frac{1}{64} \int \frac{d^d \mathbf{q}_1 d^d \mathbf{q}_2}{(2\pi)^{2d}} \int dy \frac{e^{-2(|\mathbf{p}|+|\mathbf{q}_1|)|y|}}{|\mathbf{q}_1|^2 |\mathbf{q}_2| |\mathbf{q}_1 + \mathbf{q}_2|^2} \\
&= -\frac{1}{64} \int \frac{d^d \mathbf{q}_1 d^d \mathbf{q}_2}{(2\pi)^{2d}} \frac{1}{|\mathbf{q}_1|^2 |\mathbf{q}_2| |\mathbf{q}_1 + \mathbf{q}_2|^2 (|\mathbf{p}| + |\mathbf{q}_1|)}. \tag{A.13}
\end{aligned}$$

We use (A.8) to integrate over \mathbf{q}_2 and (A.9) to integrate over \mathbf{q}_1 . We obtain

$$\begin{aligned}
U_2 &= \frac{\mu^{-2\varepsilon}}{32(4\pi)^d} \frac{\Gamma(\frac{d-1}{2})\Gamma(\frac{d-2}{2})\Gamma(\frac{3-d}{2})\Gamma(1-2d)\Gamma(2d)}{\Gamma(\frac{1}{2})\Gamma(d-\frac{3}{2})\Gamma(\frac{d}{2})} \\
&= -\frac{\mu^{-2\varepsilon}}{512\pi^4} \left(\frac{1}{\varepsilon^2} + \frac{3-\gamma+\ln\pi}{\varepsilon} + \mathcal{O}(\varepsilon^0) \right). \tag{A.14}
\end{aligned}$$

For the corresponding beta function coefficient we find $2a_{U_2} = \frac{1}{4}$.

The integral U_4 We have

$$\begin{aligned}
U_4 &= -\frac{1}{64} \int \frac{d^d \mathbf{q}_1 d^d \mathbf{q}_2}{(2\pi)^{2d}} \int dy \frac{e^{-2(|\mathbf{q}_1|+|\mathbf{p}|)|y|}}{|\mathbf{q}_1|^3 |\mathbf{q}_2| |\mathbf{q}_1 + \mathbf{q}_2|} \\
&= -\frac{1}{64} \int \frac{d^d \mathbf{q}_1 d^d \mathbf{q}_2}{(2\pi)^{2d}} \frac{1}{|\mathbf{q}_1|^3 |\mathbf{q}_2| (|\mathbf{q}_1 + \mathbf{q}_2| (|\mathbf{q}_1| + |\mathbf{p}|))} \\
&= \frac{\mu^{-2\varepsilon}}{32(4\pi)^d} \frac{\Gamma(\frac{d-1}{2})^2 \Gamma(\frac{2-d}{2}) \Gamma(2d) \Gamma(1-2d)}{\Gamma(\frac{d}{2}) \Gamma(\frac{1}{2})^2 \Gamma(d-1)} \\
&= \frac{\mu^{-2\varepsilon}}{1024\pi^4 \varepsilon} + \mathcal{O}(\varepsilon^0), \tag{A.15}
\end{aligned}$$

where we first integrated over \mathbf{q}_2 using (A.8) and then over \mathbf{q}_1 using (A.9). For the corresponding beta function coefficient we then obtain $2a_{U_4} = -\frac{1}{8}$.

The integral K_2 We have

$$\begin{aligned}
K_2 &= -\frac{1}{128|\mathbf{p}|} \int \frac{d^d \mathbf{q}_1 d^d \mathbf{q}_2}{(2\pi)^{2d}} \int dy \frac{e^{-2(|\mathbf{q}_1|+|\mathbf{p}|)|y|}}{|\mathbf{q}_1|^2 |\mathbf{q}_2| |\mathbf{q}_1 + \mathbf{q}_2|} \\
&= -\frac{1}{128|\mathbf{p}|} \int \frac{d^d \mathbf{q}_1 d^d \mathbf{q}_2}{(2\pi)^{2d}} \frac{1}{|\mathbf{q}_1|^2 |\mathbf{q}_2| |\mathbf{q}_1 + \mathbf{q}_2| (|\mathbf{q}_1| + |\mathbf{p}|)} \\
&= -\frac{\mu^{-2\varepsilon}}{128(4\pi)^d} \frac{\Gamma(\frac{d-1}{2})^2 \Gamma(\frac{2-d}{2}) \Gamma(2d-4) \Gamma(5-2d)}{\Gamma(\frac{d}{2}) \Gamma(\frac{1}{2})^2 \Gamma(d-1)} \\
&= -\frac{\mu^{-2\varepsilon}}{4096\pi^4 \varepsilon} + \mathcal{O}(\varepsilon^0), \tag{A.16}
\end{aligned}$$

where we first integrated over \mathbf{q}_2 using (A.8) and then over \mathbf{q}_1 using (A.9). For the corresponding beta function coefficient we obtain $2a_{K_2} = \frac{1}{16}$.

References

- [1] K. G. Wilson & M. E. Fisher, “*Critical exponents in 3.99 dimensions*”, *Phys. Rev. Lett.* **28**, 240 (1972).
- [2] M. A. Vasiliev, “*Nonlinear equations for symmetric massless higher spin fields in (A)dS(d)*”, *Phys. Lett. B* **567**, 139 (2003), [hep-th/0304049](#).
- [3] M. Moshe & J. Zinn-Justin, “*Quantum field theory in the large N limit: A Review*”, *Phys. Rept.* **385**, 69 (2003), [hep-th/0306133](#).
- [4] A. M. Polyakov, “*Nonhamiltonian approach to conformal quantum field theory*”, *Zh. Eksp. Teor. Fiz.* **66**, 23 (1974).
- [5] F. Kos, D. Poland & D. Simmons-Duffin, “*Bootstrapping the $O(N)$ vector models*”, *JHEP* **1406**, 091 (2014), [arXiv:1307.6856 \[hep-th\]](#).
- [6] D. Poland, S. Rychkov & A. Vichi, “*The Conformal Bootstrap: Theory, Numerical Techniques, and Applications*”, *Rev. Mod. Phys.* **91**, 015002 (2019), [arXiv:1805.04405 \[hep-th\]](#).
- [7] A. Pelissetto & E. Vicari, “*Critical phenomena and renormalization group theory*”, *Phys. Rept.* **368**, 549 (2002), [cond-mat/0012164](#).
- [8] H. Osborn & A. Stergiou, “*Seeking fixed points in multiple coupling scalar theories in the ε expansion*”, *JHEP* **1805**, 051 (2018), [arXiv:1707.06165 \[hep-th\]](#).
- [9] S. Rychkov & A. Stergiou, “*General Properties of Multiscalar RG Flows in $d = 4 - \varepsilon$* ”, *SciPost Phys.* **6**, 008 (2019), [arXiv:1810.10541 \[hep-th\]](#).
- [10] H. Osborn & A. Stergiou, “*Heavy handed quest for fixed points in multiple coupling scalar theories in the ε expansion*”, *JHEP* **2104**, 128 (2021), [arXiv:2010.15915 \[hep-th\]](#).
- [11] D. M. McAvity & H. Osborn, “*Conformal field theories near a boundary in general dimensions*”, *Nucl. Phys. B* **455**, 522 (1995), [cond-mat/9505127](#).

- [12] M. Billò, V. Gonçalves, E. Lauria & M. Meineri, “*Defects in conformal field theory*”, *JHEP* **1604**, 091 (2016), [arXiv:1601.02883 \[hep-th\]](#).
- [13] L. Sigl & W. Fenzl, “*Order-parameter exponent β_1 of a binary liquid mixture at a boundary*”, *Phys. Rev. Lett.* **57**, 2191 (1986).
- [14] L. Mailänder, H. Dosch, J. Peisl & R. Johnson, “*Near-surface critical x-ray scattering from Fe_3Al* ”, *Phys. Rev. Lett.* **64**, 2527 (1990).
- [15] B. Burandt, W. Press & S. Haussühl, “*Near-surface X-ray critical scattering from a NH_4Br ($11\bar{0}$) surface*”, *Phys. Rev. Lett.* **71**, 1188 (1993).
- [16] S. Alvarado, M. Campagna & H. Hopster, “*Surface magnetism of Ni (100) near the critical region by spin-polarized electron scattering*”, *Phys. Rev. Lett.* **48**, 51 (1982).
- [17] R. F. Chang, H. Burstyn & J. V. Sengers, “*Correlation function near the critical mixing point of a binary liquid*”, *Phys. Rev. A* **19**, 866 (1979).
- [18] P. Damay, F. Leclercq & P. Chieux, “*Critical scattering function in a binary fluid mixture: A study of sodium-deuteroammonia solution at the critical concentration by small-angle neutron scattering*”, *Phys. Rev. B* **40**, 4696 (1989).
- [19] P. Damay, F. Leclercq, R. Magli, F. Formisano & P. Lindner, “*Universal critical-scattering function: An experimental approach*”, *Phys. Rev. B* **58**, 12038 (1998).
- [20] A. J. Bray & M. A. Moore, “*Critical behaviour of semi-infinite systems*”, *Journal of Physics A: Mathematical and General* **10**, 1927 (1977).
- [21] K. Ohno & Y. Okabe, “*The $1/N$ expansion for the N vector model in the semi-infinite space*”, *Prog. Theor. Phys.* **70**, 1226 (1983).
- [22] G. Gompper & H. Wagner, “*Conformal invariance in semi-infinite systems: Application to critical surface scattering*”, *Zeitschrift für Physik B Condensed Mat* **59**, 193 (1985).
- [23] H. W. Diehl, “*The Theory of Boundary Critical Phenomena*”, *Int. J. Mod. Phys. B* **11**, 3503 (1997), [cond-mat/9610143](#).
- [24] M. A. Metlitski, “*Boundary criticality of the $O(N)$ model in $d = 3$ critically revisited*”, *SciPost Phys.* **12**, 131 (2022), [arXiv:2009.05119 \[cond-mat.str-el\]](#).
- [25] J. Padayasi, A. Krishnan, M. A. Metlitski, I. A. Gruzberg & M. Meineri, “*The extraordinary boundary transition in the 3d $O(N)$ model via conformal bootstrap*”, *SciPost Phys.* **12**, 190 (2022), [arXiv:2111.03071 \[cond-mat.stat-mech\]](#).
- [26] F. P. Toldin & M. A. Metlitski, “*Boundary Criticality of the 3D $O(N)$ Model: From Normal to Extraordinary*”, *Phys. Rev. Lett.* **128**, 215701 (2022), [arXiv:2111.03613 \[cond-mat.stat-mech\]](#).

- [27] A. Krishnan & M. A. Metlitski, “A plane defect in the 3d $O(N)$ model”, *SciPost Phys.* **15**, 090 (2023), [arXiv:2301.05728 \[cond-mat.str-el\]](#).
- [28] W. H. Pannell & A. Stergiou, “Line defect RG flows in the ϵ expansion”, *JHEP* **2306**, 186 (2023), [arXiv:2302.14069 \[hep-th\]](#).
- [29] S. Giombi & B. Liu, “Notes on a surface defect in the $O(N)$ model”, *JHEP* **2312**, 004 (2023), [arXiv:2305.11402 \[hep-th\]](#).
- [30] M. Trépanier, “Surface defects in the $O(N)$ model”, *JHEP* **2309**, 074 (2023), [arXiv:2305.10486 \[hep-th\]](#).
- [31] A. Raviv-Moshe & S. Zhong, “Phases of surface defects in Scalar Field Theories”, *JHEP* **2308**, 143 (2023), [arXiv:2305.11370 \[hep-th\]](#).
- [32] S. Harribey, I. R. Klebanov & Z. Sun, “Boundaries and interfaces with localized cubic interactions in the $O(N)$ model”, *JHEP* **2310**, 017 (2023), [arXiv:2307.00072 \[hep-th\]](#).
- [33] P. Cvitanovic, “Group Theory: Birdtracks, Lie’s, and Exceptional Groups”, Princeton University Press (2020).
- [34] G. ’t Hooft, “Dimensional regularization and the renormalization group”, *Nucl. Phys. B* **61**, 455 (1973).
- [35] J. Henriksson, “The critical $O(N)$ CFT: Methods and conformal data”, *Phys. Rept.* **1002**, 1 (2023), [arXiv:2201.09520 \[hep-th\]](#).
- [36] Y. Pang, J. Rong & N. Su, “ ϕ^3 theory with F_4 flavor symmetry in $6 - 2\epsilon$ dimensions: 3-loop renormalization and conformal bootstrap”, *JHEP* **1612**, 057 (2016), [arXiv:1609.03007 \[hep-th\]](#).
- [37] J. Rong & N. Su, “Bootstrapping the $\mathcal{N} = 1$ Wess-Zumino models in three dimensions”, *JHEP* **2106**, 153 (2021), [arXiv:1910.08578 \[hep-th\]](#).
- [38] P. Liendo & J. Rong, “Seeking SUSY fixed points in the $4 - \epsilon$ expansion”, *JHEP* **2112**, 033 (2021), [arXiv:2107.14515 \[hep-th\]](#).
- [39] I. Jack, H. Osborn & T. Steudtner, “Explorations in scalar fermion theories: β -functions, supersymmetry and fixed points”, *JHEP* **2402**, 038 (2024), [arXiv:2301.10903 \[hep-th\]](#).
- [40] P. Dey & A. Söderberg, “On analytic bootstrap for interface and boundary CFT”, *JHEP* **2107**, 013 (2021), [arXiv:2012.11344 \[hep-th\]](#).
- [41] F. Gliozzi, P. Liendo, M. Meineri & A. Rago, “Boundary and Interface CFTs from the Conformal Bootstrap”, *JHEP* **1505**, 036 (2015), [arXiv:1502.07217 \[hep-th\]](#).
- [42] C. Behan, L. Di Pietro, E. Lauria & B. C. Van Rees, “Bootstrapping boundary-localized interactions”, *JHEP* **2012**, 182 (2020), [arXiv:2009.03336 \[hep-th\]](#).

- [43] C. Behan, L. Di Pietro, E. Lauria & B. C. van Rees, “*Bootstrapping boundary-localized interactions II. Minimal models at the boundary*”, [JHEP **2203**, 146 \(2022\)](#), [arXiv:2111.04747 \[hep-th\]](#).
- [44] S. Shimamori, “*Conformal field theory with composite defect*”, [arXiv:2404.08411 \[hep-th\]](#).
- [45] O. Diatlyk, H. Khanchandani, F. K. Popov & Y. Wang, “*Effective Field Theory of Conformal Boundaries*”, [arXiv:2406.01550 \[hep-th\]](#).
- [46] P. Kravchuk, A. Radcliffe & R. Sinha, “*Effective theory for fusion of conformal defects*”, [arXiv:2406.04561 \[hep-th\]](#).
- [47] King’s College London, “*King’s Computational Research, Engineering and Technology Environment (CREATE)*”, <https://doi.org/10.18742/rnvf-m076>.
- [48] J. Martín-García, “*xAct: Efficient Tensor Computer Algebra for Mathematica*”, <http://www.xact.es>.
- [49] T. Nutma, “*xTras : A field-theory inspired xAct package for Mathematica*”, [Comput. Phys. Commun. **185**, 1719 \(2014\)](#), [arXiv:1308.3493 \[cs.SC\]](#).
- [50] N. N. Bogoliubov & O. S. Parasiuk, “*On the Multiplication of the causal function in the quantum theory of fields*”, [Acta Math. **97**, 227 \(1957\)](#).
- [51] W. K. Theumann & M. A. Gusmao, “*Critical exponents for ϕ^3 field models with long range interactions*”, [Phys. Rev. B **31**, 379 \(1985\)](#).